IV.2 Catalizadores de níquel y níquel-magnesia. Aplicación a la hidrogenación de dinitrilos.

El interés industrial de la gran mayoría de dinitrilos radica en su utilización para obtener especies monoamina y/o diamina que son posteriormente aplicadas a la producción de nylons [1,2]. No obstante, estudios más recientes muestran también la potencialidad de estos reactivos en otras reacciones. Así, parece factible la obtención de N-heterociclos de interés en la industria farmacéutica a partir de dinitrilos [66].

En este trabajo se han utilizado como reactivos 1,4-butanodinitrilo (succinonitrilo) y 1,6-hexanodinitrilo (adiponitrilo). La elección de los reactivos y el desarrollo del estudio de actividad catalítica se ha realizado en base a diferentes consideraciones.

El 1,4-butanodinitrilo se ha utilizado como dinitrilo modelo ya que es el dinitrilo de cadena más corta que puede dar productos de ciclación estables. Con este dinitrilo se ha realizado un estudio comparativo de la actividad catalítica de diferentes sistemas Ni-MgO.

De entre los diferentes precursores sintetizados en la primera parte del trabajo (IV.13), se escogieron los precursores catalíticos (NiOA) y NiO/MgO preparados con diferentes relaciones másicas y mediante las vías A y B ($1C_1A$, $4C_1A$, $4C_1B$, 4NA) para obtener los catalizadores que han sido probados en la reacción de hidrogenación de 1,4-butanodinitrilo en fase vapor y a presión atmosférica. Los sistemas preparados mediante la vía A conducen a sistemas sin una morfología octaédrica definida y forman solución sólida entre las fases. Sin embargo, la vía B conduce a sistemas con solución sólida pero formados por partículas homogéneas de una cierta morfología octaédrica.

El estudio de hidrogenación de 1,4-butanodinitrilo nos ha permitido establecer correlaciones entre las diferentes propiedades de los catalizadores y los resultados de actividad catalítica. Asimismo, se ha obtenido información sobre las limitaciones del montaje de reacción con el fin de poder variar diferentes parámetros externos (velocidad espacial, relaciones H_2/dinitrilo, etc.) que nos permitan optimizar los resultados de actividad catalítica y que nos den una visión amplía de los problemas de la hidrogenación catalítica en fase vapor a presión atmosférica.

A partir de los resultados del estudio con el 1,4-butanedinitrilo se ha escogido el catalizador R4C_3B que es el que presenta los mejores resultados para ser utilizado en la hidrogenación de un dinitrilo de mayor interés industrial como el 1,6-hexanodinitrilo.

Con el fin de obtener un sistema Ni-MgO con una mayor definición de la morfología octaédrica se empleó la vía preparativa C que condujo a la obtención de sistemas NiO-MgO sin formar solución sólida y de elevada definición en la morfología octaédrica. Posteriormente, se realizó un estudio de actividad catalítica para la hidrogenación de 1,6-hexanodinitrilo en fase vapor a presión atmosférica utilizando el catalizador (R4C_3B) y el catalizador obtenido del precursor preparado mediante la vía C (R4C_3C). Estos resultados han sido comparados con los resultados de actividad catalítica de un catalizador comercial de uso industrial (Raney-Ni).

Se ha realizado también un estudio de vida activa de los catalizadores Ni-MgO (R4C_3B y R4C_3C) que presentaron las mejores selectividades en los productos de interés, y se comparan con los resultados obtenidos con catalizadores sin magnesia (Raney-Ni y NiB).

Este estudio permitirá evaluar una futura viabilidad en la utilización de catalizadores Ni-MgO a escala industrial.

IV.2.1 Catatizadores de níquel y níquel-magnesia activos en la hidrogenación de 1,4-butanodinitrilo.

Journal of Catalysis 197, páginas 210-219.

doi:10.1006/jcat.2000.3084

Nickel and nickel-magnesia catalysts active in the hydrogenation of 1,4- Butanedinitrile.

Marc Serra[a], Pilar Salagre[a*], Yolanda Cesteros[a], Francisco Medina[b] and Jesús E. Sueiras[b].

[a] *Facultat de Química, Universitat Rovira i Virgili, Pl. Imperial Tarraco,1. 43005, Tarragona, Spain. e-mail: salagre@quimica.urv.es*

[b] *Escola Tècnica Superior d'Enginyeria Química, Universitat Rovira i Virgili, Pl. Imperial Tarraco,1. 43005, Tarragona, Spain*

ABSTRACT

Several NiO-MgO systems were synthesized to be studied as nickel catalysts for the hydrogenation of 1,4-butanedinitrile in the gas phase and compared with a bulk NiO of controlled morphology. All samples were characterized by XRD, BET, TPR, TPD, SEM and H_2 chemisorption techniques. The Ni-MgO systems had higher activities than the Ni bulk catalyst. The most active catalyst at all reaction temperatures was type $R4C_1B$ which had homogeneous particles of about 1000 Å, the highest metal surface area and the highest coverage with weakly-bound hydrogen. The presence of basic magnesia suppresses the condensation reactions and consequently favours the elimination of amines, and prevents catalyst deactivation.

The selectivity towards the different products not only depends on the catalytic properties but can also be modified by controlling the hydrogen/dinitrile ratio. The highest selectivity to 4-aminobutanenitrile was achieved by catalyst $R4C_1B$, with 85% at 100 % conversion and working at a space velocity of 13000 h^{-1} and 343 K. This selectivity could be increased by lowering the hydrogen/butanedinitrile ratio.

Key Words: Nickel-magnesia catalysts; magnesia; succinonitrile; dinitrile; 1,4-butanedinitrile hydrogenation.

INTRODUCTION

Hydrogenation of nitriles is one of the most widely used methods to obtain amines commercially [1,2], and production of alifatic amines has been the most important application. One interesting industrial process is the hydrogenation of 1,6-hexanedinitrile (adiponitrile) to obtain 1,6-hexanediamine which is used as a precursor in the preparation of Nylon-6,6 [3-5].

Recent studies have shown that the hydrogenation-cyclization of dinitriles is one of the new interesting research fields in organic synthesis to obtain N-heterociclyclic compounds. Nowadays, pyridine derivatives such as α- and β -picolines are used to obtain precursors of many chemical products which are important in medicine, farming and industry. These compounds have usually been prepared by aldol condensation. Prins [6] has recently proposed the catalytic hydrogenation of 2-methylglutaronitrile as an alternative process to obtain these picoline compounds. The 2-methylglutaronitrile is a by-product in the DuPont process for manufacturing adiponitrile from butadiene [6,7] and therefore, such catalytic process means that by-products can be used as raw materials.

Nitrile hydrogenation products are composed mainly of a mixture of primary, secondary, and tertiary amines [8,9]. The condensation reactions between a highly reactive intermediate imine and the primary amine always lead to the formation of such products as secondary and tertiary amines together with the primary amines [10].

The selectivity of the nitrile hydrogenation process is of great importance and depends on the properties of the starting nitrile, the catalyst used and the reaction conditions. However, the catalyst is the

most important factor [2,11]. Catalysts based on Co, Ni and Ru are mostly used to produce primary amines. Cu and Rh catalysts are mostly used to obtain secondary amines while tertiary amines can be prepared by using Pt and Pd catalysts [12-13].

Amines are usually prepared industrially in the liquid phase at high hydrogen pressures. Nickel catalysts, however, have been used at lower pressures, in the gas phase, although an excess of ammonia was essential to suppress secondary and tertiary amine formation [10,14]. Also, the addition of potassium in dopant amounts enhances the selectivity of nickel catalysts towards primary amines in adiponitrile hydrogenation [15-18].

Recently, precursors such as hydrotalcites have made it possible to vary the MgO/Al_2O_3 ratio and thus control the acidity of the catalysts [19,20]. When this ratio increases, the selectivity to primary amines in the acetonitrile hydrogenation also increases.

Double selective catalysts are required if 6-aminohexanenitrile is to be obtained selectively in the adiponitrile hydrogenation. Such catalysts lead to primary amines with only one hydrogenated nitrile group. This selectivity could be related to the crystallinity of the active phase. In this respect, $Ni/\alpha\text{-}Al_2O_3$ catalysts with nickel particles of octahedral morphology [21] and crystalline Raney nickel catalysts [22] have shown very high selectivity to the monoamine compound. It has also been observed that the morphology and size of nickel particles are related to the method used to prepare NiO-MgO systems [23].

In this study, we propose that Ni-MgO systems with nickel metallic phases of different crystallinity can be used to control the selectivity to monoamine or to cyclic derivatives. Different magnesia sources will suppress the condensation reactions and consequently the

lifetime of the catalysts will increase. The catalytic tests were performed in the gas phase at 1atm pressure for the hydrogenation of 1,4-butanedinitrile.

EXPERIMENTAL

Catalysts preparation

NiO of octahedral morphology was prepared according to Estelle et al. [24]. It consists in thermally decomposing $Ni(NO_3)_2.6H_2O$ at 373 K for fourteen days in order to obtain $Ni_3(NO_3)_2(OH)_4$ as a single phase which is then calcined at 623 K for 40 minutes to obtain the NiO sample, referred to as NiOA. The corresponding catalyst was obtained by reduction under H_2 at 673 K for 4h. This sample was named NiA.

Three NiO-MgO samples were prepared by modifying the MgO source and/or the preparative procedure according to the method previously described [23] which is briefly summarized as follows. The NiO/MgO weight ratio was 4:1 for all samples (referred to as 4). Two MgO sources were used: a commercial MgO_{C1} (BET surface area 223 m^2g^{-1}, referred to as C_1) and a magnesia obtained by thermal decomposition of magnesium nitrate hexahydrate MgO_N (BET surface area 2.5 m^2g^{-1} and referred to as N).

Two preparative procedures were performed: path A and path B (referred to as A and B, respectively). Path A consisted of a direct calcination of a $Ni(NO_3)_2{\cdot}6H_2O$ and MgO mixture at 673 K (samples $4C_1A$ and 4NA). In the path B, a controlled thermolysis of a nickel nitrate and MgO_{C1} mixture was carried out to obtain $Ni_3(NO_3)_2(OH)_4$. This sample was later calcined at a lower temperature (523 K) than in case A (sample $4C_1B$).

Finally, all samples obtained by path A and B were reduced under pure H_2 at 673 K for 6h (catalysts $R4C_1A$, R4NA and $R4C_1B$).

Air-free sampling

After the reduction step, the catalysts were always handled under air-free conditions. The samples were transferred in degassed isooctane under a hydrogen atmosphere at room temperature. The isooctane surface-impregnated samples were further isolated from the air either by gold film for the scanning electron microscopy (SEM) study or by sticky tape for X-ray diffraction (XRD) monitoring. A glove box was used for mounting. The catalytic activity was measured in situ, in the same reactor after reduction, where gas purges, positive gas pressures and Schlenk techniques were used when necessary.

BET surface areas

Surface areas were calculated from the nitrogen adsorption isotherms at 77 K using a Micromeritics ASAP 2000 surface analyser and a value of 0.164 nm^2 for the cross-section of the nitrogen molecule.

X-ray diffraction (XRD)

Powder X-ray diffraction patterns of the different samples were obtained with a Siemens D5000 diffractometer using nickel-filtered Cu Kα radiation. Samples were dusted on double-sided sticky tape and mounted on glass microscope slides. The patterns were recorded over a range of 2θ angles from 10º to 90º and crystalline phases were

identified using the Joint Committee on Powder Diffraction Standards (JCPDS) files.

The XRD patterns of MgO are very similar to those of NiO. The peak positions corresponding to 2θ angles (with the relative intensities in parentheses), taken from the JCPDS files, are: 36.95 (10), 42.91 (100), 62.31 (52), 74.68 (4) and 78.61 (12) for the MgO phase and 37.28 (91), 43.30 (100), 62.92 (57), 75.44 (16) and 79.39 (13) for the NiO phase. Both 2θ peaks are assigned to the faces (1 1 1), (2 0 0), (2 2 0), (3 1 1) and (2 2 2), respectively. The 2θ angles and the relative intensities (in parentheses) are 44.51 (100), 51.85(42), 76.36 (21) for the Ni phase.

This technique was also used to determine the reduction degree (α) of the catalysts by means of the Rietveld method [25]. This method implies quantitative phase analysis of multicomponent mixtures from the X-ray powder diffraction data. It is only necessary to know the crystal structure of each phase of interest.

Temperature-programmed reduction (TPR)

Temperature-programmed reduction studies (TPR) were carried out in a Labsys/Setaram TG DTA/DSC thermobalance equipped with a 273-1273 K programmable temperature furnace. The accuracy was ±1μg.

Each sample (90 mg) was first heated at 423 K in an Ar flow ($80cm^3min^{-1}$) until no change of weight was detected. Then, the sample was heated in a 5 vol%H_2/Ar flow ($80cm^3min^{-1}$) from 423 K to 1173 K

at a rate of 5K min^{-1} and maintained at 1173 K until the reduction process had finished.

Scanning electron microscopy (SEM)

Scanning electron micrographs were obtained with a JEOL JSM6400 scanning microscope operating at an accelerating voltage in the range 30-35 kV, a work distance (w.d.) between 7-9mm and at a magnification factor of 40000 to 50000.

Temperature-programmed desorption (TPD)

TPD spectra were obtained with a FISONS QTMD 150 gas desorption unit equipped with a 273-1273 K programmable temperature furnace and a mass spectrometer detector.

Samples were reduced in a pure H_2 flow (80 cm^3min^{-1}) from room temperature at 1 $Kmin^{-1}$ up to 673 K. They were isothermally maintained at this last temperature for 4 h to obtain the catalyst NiA and for 6 h to obtain catalysts $R4C_1A$, $R4C_1B$ and R4NA. The samples were then cooled down to room temperature in the hydrogen flow, evacuated for 1 h at low pressures (<1 Pa) and heated at a rate of 10 K min^{-1} up to 1123 K. The hydrogen desorption was detected with the mass spectrometer.

Hydrogen chemisorption

Hydrogen chemisorption was measured with a Micromeritics ASAP 2010C instrument equipped with a turbomolecular pump. Samples had been reduced previously under the same conditions in which the catalysts had been prepared. After reduction, the

chemisorbed hydrogen was removed in a stream of 30 ml min^{-1} of He for 30 min at 683 K. The sample was subsequently cooled to 303 K in the same He stream. The chemisorbed hydrogen was analysed at 303 K. The nickel surface area was calculated assuming a stoichiometry of one hydrogen molecule per two surface nickel atoms and an atomic cross-sectional area of $6.49x10^{-20}$ m^2/Ni atom.

Determination of the catalytic activity

The gas phase hydrogenation of 1,4-butanedinitrile was studied in a tubular fixed-bed flow reactor heated by an oven equipped with a temperature control system.

The reactor was filled with catalyst (500 mg) and the catalytic reaction for 1,4-butanedinitrile vapour at 353 K was measured at 1 atm pressure, using space velocities between 6500-13000 h^{-1} and reaction temperatures between 343-453 K.

No diffusional retardation was observed as the residence times lie on the linear portion of the curve obtained when plotting conversion against residence time for different catalyst volumes.

Reaction products were analysed by an on-line gas-chromatograph HP 5890 equipped with a 30 m cappillar column "commercial Rtx-5 amine" and a flame ionization detector.

Conversion and selectivity were defined by the following equations: conversion (%)= [moles of 1,4-butanedinitrile consumed] x 100 / [moles of 1,4-butanedinitrile charged]; selectivity (%) = [moles of one product of reaction] x 100 / [moles of 1,4-butanedinitrile consumed]. The carbon mass balance of the process was always held.

RESULTS AND DISCUSSION

X-ray diffraction (XRD)

Sample NiOA shows peaks which can be attributed to crystalline NiO whereas the powder diffraction patterns of the NiO-MgO systems [23] show peaks which correspond to a crystalline solid solution of the components.

TABLE 1

Characterization of catalysts

	NiA	R4C$_1$A	R4NA	R4C$_1$B
Crystalline phases	Ni	Ni	Ni	Ni
(XRD)		NiO-MgO	NiO-MgO	NiO-MgO
Reduction degree	1	0.12	0.56	0.29
α(XRD)[a]				
Metallic area [b] (m^2g^{-1})	0.2	1.6	2.0	4.1

[a] Reduction degree obtained by using the Rietveld method [25]
[b] Metal surface area, calculated from H_2 chemisorption.

Table 1 shows the crystalline phases obtained by XRD for the catalysts. The NiA catalyst contains crystalline nickel as a single phase. However, the reduced catalysts Ni-MgO (samples R4C$_1$A, R4NA and R4C$_1$B) have powder diffraction patterns corresponding to two phases: a crystalline solid solution phase and a less crystalline Ni phase (see Table 1). The detection by XRD of a solid solution phase for the catalysts indicates that the reduction of NiO is not complete. Therefore,

the presence of magnesia hinders the reduction process, in agreement with what has been reported by Arena et al. [26-28].

The degrees of reduction (α) were determined from the corresponding diffraction patterns using the Rietveld method [25] for all catalysts (Table 1). The NiA catalyst had the highest degree of reduction, as expected.

When path A was used to prepare the Ni-MgO catalysts, the degrees of reduction were lower than when path B was used (0.12 for $R4C_1A$ and 0.29 for $R4C_1B$) for the same magnesia source. The reduction degree of catalyst $R4C_1A$ is lower because the diffusion between the NiO and MgO phases (which hinders the reduction of NiO) is better at the higher calcination temperature used in path A (673 K) than in path B (523 K).

The reduction degree for catalyst R4NA is higher (α=0.56) than for catalyst $R4C_1A$ (α=0.12). This is in agreement with the diffusion problems observed (23) for the MgO_N which had larger particles (crystallite sizes >1200 Å) than the MgO_{C1} (crystallite sizes of 47 Å). TPR results, commented below, confirm this behaviour.

BET surface areas

The surface area of the NiOA sample is 11 m^2g^{-1} and for the NiO-MgO systems range between 24 and 36 m^2g^{-1}. After reduction of the catalytic precursors, a small decrease in surface areas has been observed due to the formation of a new crystalline and more compact Ni phase. The low surface area of the catalysts $R4C_1A$ and $R4C_1B$ (and their catalyst precursors) contrast with the high area of its MgO_{C1}

source (223 m^2g^{-1}). This is in agreement with the results reported by Anderson et al. [29] who observed considerable sintering of high-surface area magnesia samples in the presence of low amounts of water vapour at the calcination temperatures used.

Temperature-programmed reduction (TPR)

The reducibility of the NiOA sample was estimated by TPR considering its initial reduction temperature in order to be compared with the initial reduction temperature obtained for the NiO-MgO systems, previously [23]. The interest of these reducibility studies is to confirm the differences in the degrees of reduction (α) observed by XRD for the four catalysts, as mentioned above. The initial reduction temperature values (T_R) are 583, 598, 604 and 613 K for the samples NiOA, 4NA, $4C_1B$ and $4C_1A$, respectively. The initial reduction temperature of the NiOA sample (583 K) is lower than that of the systems prepared with magnesia whereas its reduction degree (α=1) is higher (see Table 1). This confirms that the interaction between NiO and MgO leads to the formation of a NiO-MgO solid solution for these systems [27-28]. This hinders the reduction of NiO. Comparing the three Ni-MgO catalysts, the catalyst which has the highest reduction degree (R4NA) is that whose precursor showed the lowest initial reduction temperature.

Scanning electron microscopy (SEM)

Scanning electron microscopy was used to monitor the morphology and particle size of the different precursors and their

reduced forms. Figures 1, 2 and 3 show the micrographs of the NiOA, $4C_1A$ and $4C_1B$ samples, respectively.

The NiO sample and its reduced form, NiA, appear to have the same homogeneous octahedral particles with dimensions around 2500 Å. Therefore, the use of $Ni_3(NO_3)_2(OH)_4$ as a single precursor of NiO phase becomes a good method to obtain homogeneous octahedral particles in a reproducible way. This is in agreement with what has been reported by J.Estelle et al.[24].

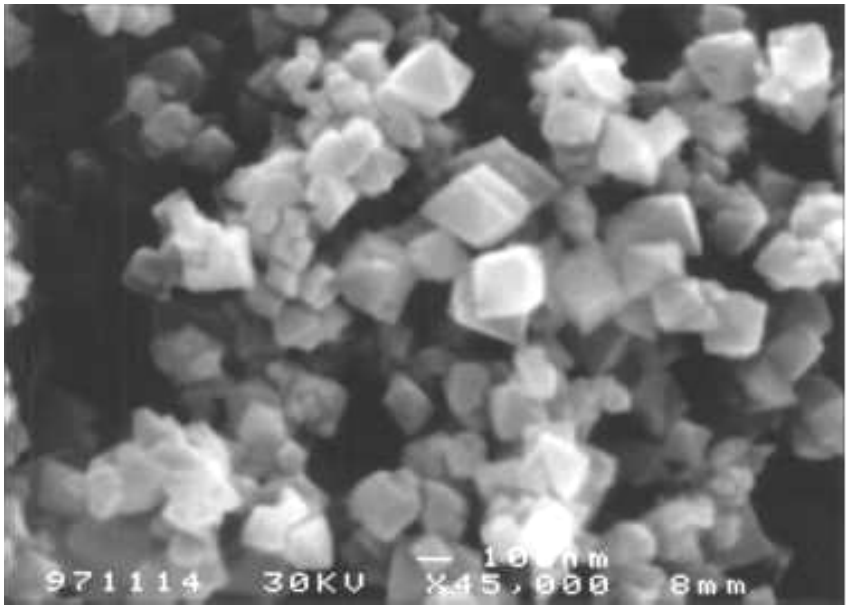

FIG. 1. Scanning electron micrograph of precursor NiOA.

For the NiO/MgO systems, different paths of preparation lead to samples with different morphologies and particle size distributions. The

sample prepared via path B is highly homogenous and has small particles (around 1000Å) with non-well defined octahedral forms. In contrast, the sample prepared via path A has spherical particles between 1000 and 10000Å. Ni-MgO catalysts do not show significant differences with respect to their catalytic precursors

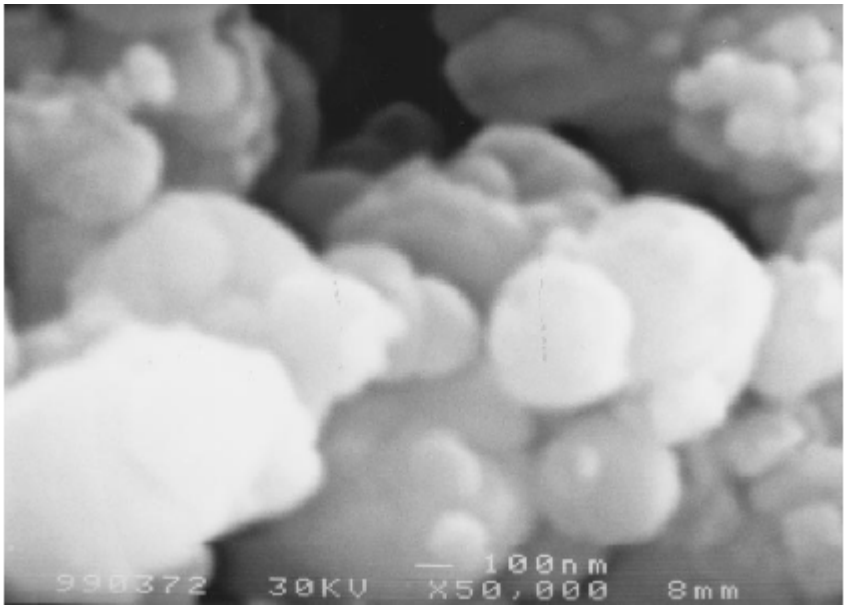

FIG. 2. Scanning electron micrograph of precursor $4C_1A$.

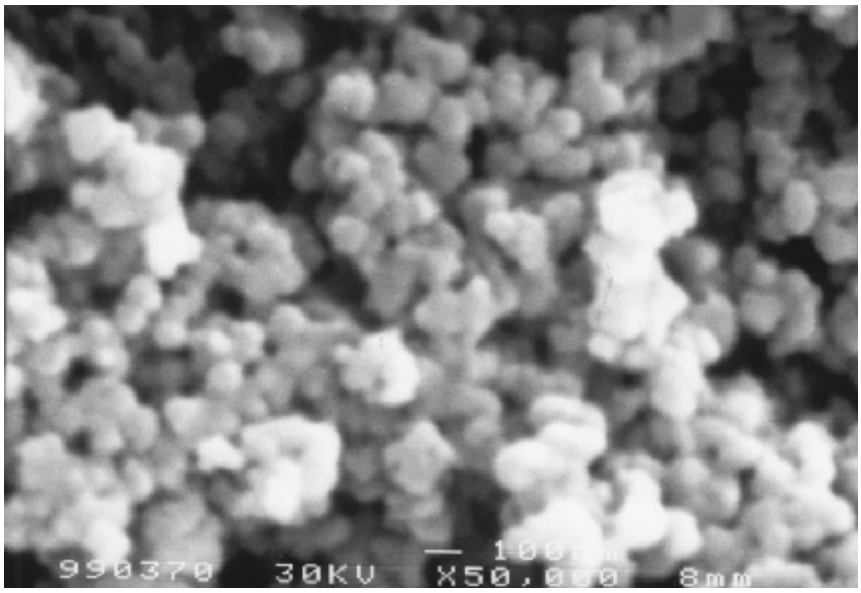

FIG. 3. Scanning electron micrograph of precursor $4C_1B$.

Temperature-programmed desorption (TPD)

To obtain information about their active sites, temperature-programmed desorption of hydrogen was performed for all the catalysts. The mechanisms of adsorption/desorption of hydrogen are extremely complex [30-51], especially when dealing with supported catalysts. This is because phenomena related to the interaction between the active phase and the support can interfere although highly complicated TPD-spectra have been also obtained for pure metal catalysts [43]. The number and population distribution of adsorbed species depend on many factors: how the catalyst was prepared, the kind of support used and the experimental conditions of the measurement such as the weight of the sample examined, the flow rate of the carrier gas, the use of ultra-high vacuum (UHV) or the shape of the reactor system which affect conditions for removal of desorbed hydrogen.

TABLE 2

Top temperatures in the H_2 TPD spectra for catalysts NiA, $R4C_1A$, R4NA and $R4C_1B$.

Catalysts	Position of peak maxima		
	T_D < 700 K		T_D > 700 K
NiA	476(w)	545(w)	821(w)
$R4C_1A$	396(m)	600(w)	-
R4NA	435(m)	687(s)	811(w)
$R4C_1B$	450(s)	634(m)	825(w)

s= strong; m= medium; w= weak.

Table 2 summarizes the hydrogen desorption temperature of the peak maxima for catalysts NiA, $R4C_1A$, R4NA and $R4C_1B$. TPD-plots show two peaks in the low-temperature region (with maxima at 400-475 K and 545-685 K, respectively) for all catalysts and one peak in the high-temperature region (with maxima at 810-825 K) for catalysts NiA, R4NA and $R4C_1B$. The low temperature region has been associated with different adsorption states of the hydrogen for other nickel catalysts [41, 50-51]. Several authors attribute the occurrence of the high-temperature peaks to hydrogen spillover taking place during high-temperature (above 773 K) treatments of the catalysts [30, 42]. Their arguments cannot be applied to the NiA catalyst which also shows a peak at 821 K. Therefore, a more probable explanation, for all catalysts, is that the high-temperature peak is associated with other adsorption states of hydrogen (due to a difference in morphology and size of the nickel particles), that we also observed for other nickel catalysts [50-51].

With all catalysts hydrogen mainly desorbed at low temperatures (< 700 K). An important point to emphasize is that H_2 populations of the low-temperature peaks are higher for the systems containing magnesia than for the pure nickel catalyst (NiA). This may be related to the higher metallic area obtained for the systems with magnesia (see Table 1) and especially to the presence of specific active sites. Therefore, there will be a greater amount of hydrogen available at the reaction temperatures for the Ni-MgO catalysts.

In the reaction mechanisms proposed in the literature for the hydrogenation of dinitrile compounds [8], different reaction products can be obtained if different amounts of hydrogen are consumed. The production of monoamine demands the lowest hydrogen consumption. This fact together with the possibility to correlate the binding strength of the chemisorbed hydrogen with the activity for a specific reaction, as has been reported for some authors [41, 50-52], give interest about the use of TPD results in the interpretation of the catalytic activity.

Catalytic Activity

Table 3 shows conversions and selectivities for hydrogenation of 1,4-butanedinitrile on nickel and nickel/magnesia catalysts (NiA, R4C$_1$A, R4NA, R4C$_1$B) under the conditions given in the section Experimental. The activity of the two pure magnesia samples was also tested and they showed to be catalytically inactive under the reaction conditions studied.

As Table 3 shows, the reaction products were: 4-aminobutanenitrile, 1,4-butanediamine, pyrrolidine, 1-pyrroline, cracking and condensation species. The selectivities towards these reaction products depend on the catalyst used. This dependence has

been studied by optimizing the reaction conditions (reaction temperature, space velocity and H_2/dinitrile ratio).

High molecular weight products are obtained in higher amounts when the catalyst is used without magnesia (NiA) at a low space velocity (6500 h^{-1}) and at high temperatures (473-453 K). On the other hand, nickel-magnesia catalysts hardly produce any condensation products and consequently they do not undergo catalyst deactivation. This is probably a consequence of the basic character of magnesia which favours the elimination of amines and prevents secondary reactions. These condensation products have been described by Prins [6] as dimers obtained as a result of an intermolecular amine-imine condensation reaction. However, if these basic catalysts are used at low space velocity (6500 h^{-1}) and high temperatures (453-423 K), cracking products are obtained. The catalyst which provides most cracking products is the catalyst one with the highest metallic area, $R4C_1B$, (see Table 1) and the highest amount of hydrogen desorbed at the reaction temperatures studied (453-343 K).

This catalyst is the most active (100% conversion) at all temperatures and space velocities used.

TABLE 3
Catalytic behaviour of four nickel catalysts as influenced by the Space Velocity and the Reaction Temperature.

Catalyst	Space velocity (h^{-1})	Reaction temp (K)	Conversion (%)	Selectivity (%)					
				4-Aminobutanenitrile	1,4-Butanediamine	Pyrrolidine	1-Pyrroline	Cracking products	Condensation products
NiA	6500	473	100	0	1	16	55	0	28
	6500	453	100	9	1	13	52	0	25
	6500	393	100	49	0	0	46	0	5
	9750	403	78	61	0	0	35	0	4
	13000	403	45	77	0	0	20	0	3
R4C$_1$A	6500	453	100	0	0	71	3	23	3
	13000	453	100	0	0	76	18	5	1
	13000	403	100	4	16	30	46	0	4
	13000	383	99	16	23	36	23	0	2
	13000	353	84	56	7	0	32	0	5
R4NA	6500	453	100	0	0	36	0	64	0
	6500	433	100	0	0	59	20	21	0
	13000	403	100	23	17	7	53	0	0
	13000	383	100	60	18	0	20	0	0
	13000	363	93	68	0	0	28	0	0
R4C$_1$B	6500	453	100	0	0	0	0	100	0
	6500	423	100	0	0	72	0	28	0
	6500	363	100	19	15	0	66	0	0
	13000	403	100	41	0	0	56	0	3
	13000	343	100	85	0	0	12	0	3

Formation of 4-aminobutanenitrile and 1,4-butanediamine

All the catalysts showed low selectivities towards 1,4-butanediamine. The NiA catalyst hardly produces any of this diamine while the selectivity to the monoamine, 4-aminobutanenitrile (77%), is highest at the lowest conversion value (45%), working at a space velocity of 13000 h^{-1} and a reaction temperature of 403 K.

However, the basic Ni-MgO catalysts produced low amounts of the diamine (selectivity<24%) and conversions and selectivities towards 4-aminobutanenitrile were high. The most active (100%) and selective catalyst to 4-aminobutanenitrile (85%) was type $R4C_1B$. This result was obtained when working at the same space velocity as with the NiA catalyst but at a lower reaction temperature (343 K).

The main difference between the two types of systems is their activity: the Ni-MgO catalysts are more active than the NiA. This means that the nickel-magnesia systems can be used at lower reaction temperatures in which cyclization is not favoured. This kind of catalysts allows to increase the selectivity to monoamine without a significant loss of conversion.

The fact that the highest activity was found for catalyst $R4C_1B$ at 343 K is probably related to the presence of one intense hydrogen TPD peak with a maximum at 450 K (see Table 2). This provides enough desorbed hydrogen at this reaction temperature for the monoamine to be selectively obtained with high conversion values (100%).

The NiA catalyst probably has a lower activity because there is less hydrogen available at lower reaction temperatures (catalyst NiA has a weak desorption peak with a maximum at 476 K) and additionally it is partially deactivated by the condensation products generated, as mentioned above.

In a previous study [21], the selective hydrogenation of one nitrile group was related to the presence of a considerable number of octahedral crystal sites. Our experiments have confirmed this since no diamine was observed when the nickel catalyst (NiA) was used. In contrast, the Ni-MgO catalysts may provide diamine as a minor product because the morphology of the nickel particles do not show well defined faces, as observed by SEM and as confirmed by XRD.

Formation of pyrrolidine and 1-pyrroline

The NiA catalyst shows low selectivities to pyrrolidine. The highest value (16%) was obtained working at 473 K and a space velocity of 6500h^{-1} at 100 % conversion. All Ni-MgO systems provide higher selectivities to pyrrolidine than the NiA catalyst. Catalyst R4C_1A has a 76% at 453 K and 13000h^{-1} and catalyst R4C_1B has a 72% at 423 K and 6500h^{-1} for a 100 % of conversion for both catalysts.

The NiA catalyst shows the highest selectivity to 1-pyrroline (55%) at the highest reaction temperature tested (473 K) and at a space velocity of 6500h^{-1} for a 100% of conversion. However, catalysts containing magnesia show the highest 1-pyrroline selectivities between 46-66% at a conversion of 100% at lower reaction temperatures (363 and 403 K).

The most active catalyst, R4C_1B, gave the highest selectivity to 1-pyrroline: 66% at 363 K whereas R4C_1A and R4NA, which are less active, gave the highest values to 1-pyrroline (46% and 53 %, respectively) at 403 K. For these catalysts, at lower temperature the amount of hydrogen available probably decreases, and consequently the formation of the less hydrogenated specie , monoamine, increases.

Pyrrolidine and 1-pyrroline are amine and imine cyclic compounds, respectively.

The formation of the imine probably needs lower amounts of hydrogen if both products are obtained from the same intermediate compound (4-aminobutaneimine). In order to investigate how hydrogen influences the production of pyrrolidine and 1-pyrroline, several experiments were performed with catalyst R4C$_1$B varying the H_2/1,4-butanedinitrile ratio and maintaining the same total flow (by dilution with argon) at a temperature of 423 K and a space velocity of 6500 h^{-1}.

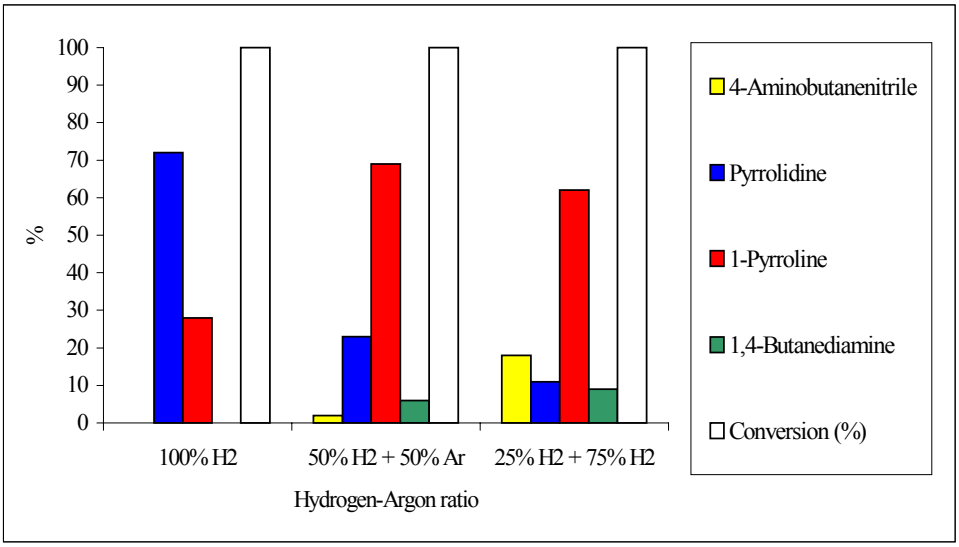

The results are shown in Fig.4.

* All experiments have been obtained at 423 K reaction temperature and at a space velocity of 6500 h^{-1}.

FIG. 4 Product selectivities for the hydrogenation of 1,4-butanedinitrile on R4C$_1$B catalyst as a function of hydrogen/1,4-butanedinitrile ratio. (The modification of these ratios has been realized by diluting hydrogen with argon.)

When 100 % of H_2 was used, the selectivity to pyrrolidine was high (72 %), when hydrogen was diluted with 50% Ar, the selectivity to 1-pyrroline clearly increased (69%). Nevertheless, a further decrease in the amount of hydrogen in the total flow (25 % H_2, 75% Ar) did not significantly change the selectivity to 1-pyrroline but there was an increase in the selectivity to 4-aminobutanenitrile (18%).

These results enabled us to propose the scheme 1 which could explain the relative formation of 1-pyrroline, pyrrolidine and 4-aminobutanenitrile in function of the availability of hydrogen in the reaction conditions. Once the aminoimine intermediate has been obtained, there are two possible side reactions: a ring-closure of the intermediate with loss of ammonia and uptake of one H_2 and a ring-closure with the loss of ammonia only. The second side reaction is probably only possible if the proportion of hydrogen in the total flow is decreased. It is of considerable importance that 4-aminobutanenitrile appeared at the lowest H_2/Ar ratio amount (see Fig.4). Hence, when less hydrogen is available, a higher selectivity to 1-pyrroline will be found.

Finally, under more diluted conditions more 4-aminobutanenitrile will be formed, even at high reaction temperatures.

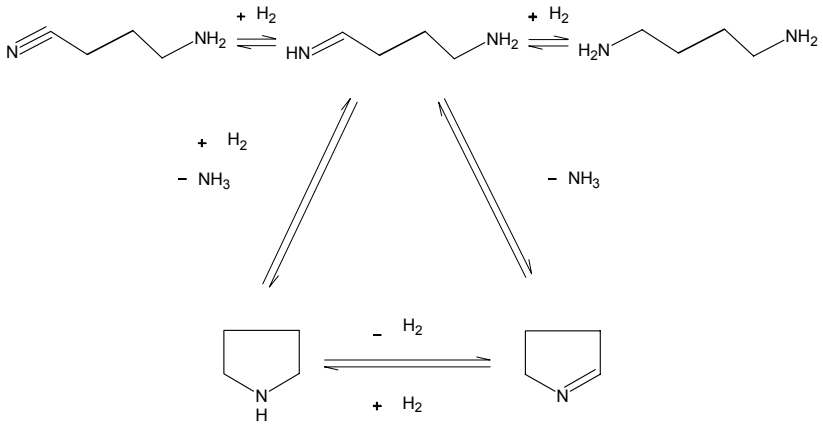

Scheme 1. Pyrrolidine and 1-pyrroline obtained by catalytic hydrogenation of 1,4-butanedinitrile (succinonitrile).

CONCLUSIONS

Several nickel-magnesia catalysts have been prepared by varying the magnesia source and the preparative method. Their performance has been compared with the behaviour of a nickel catalyst of octahedral morphology in the hydrogenation of 1,4-butanedinitrile.

All samples were structurally characterized by the application of BET, XRD, TPR, SEM, H_2 chemisorption and TPD techniques. XRD was used to identify the solid solutions obtained for all the NiO-MgO catalyst precursors and the catalysts. The NiA catalyst contained nickel only crystalline phase and all the Ni-MgO catalysts consisted of Ni and a NiO-MgO solid solution. XRD combined with TPR, enabled us to establish the sequence of reducibility of the catalyst precursors: NiOA>4NA>4C_1B>4C_1A.

SEM showed homogeneous octahedral crystallites for the NiA catalyst, whereas the micrographs obtained for the systems containing magnesia showed nickel particles with non-well defined faces, the homogeneity and sizes of which depended on the preparative path used. The NiO-MgO prepared by path B gave rise to a homogeneous system with particle sizes of around 1000 Å.

The Ni-MgO catalysts showed higher activities than the NiA catalyst. This may be due to their higher metal surface areas and hence the greater amount of available chemisorbed hydrogen (H_2 TPD results). R4C_1B was the most active catalyst under all reaction conditions studied. This is because its metal surface area was the highest (4.1 m^2g^{-1}) as well as its population of weakly bound H_2.

In the nickel-magnesia catalysts, the presence of MgO suppresses the condensation reactions and consequently there is no catalyst deactivation, probably due to the basic character of magnesia which favours the elimination of amines and prevents secondary reactions.

The selectivity towards cyclic products (pyrrolidine and 1-pyrroline) can be modified by controlling the space velocity, the reaction temperature and the hydrogen/adiponitrile ratio. High temperatures and low space velocities were required to obtain pyrrolidine. A decrease in the hydrogen/1,4-butanedinitrile ratio involves an increase in the selectivity to 1-pyrroline.

Diamine was absent in the product stream when the NiA catalyst was used but it was detected as a minor product when the Ni-MgO catalysts were used. This may be due to the higher crystallinity of the nickel phase in the NiA catalyst.

Catalyst R4C_1B shows the highest selectivity to 4-aminobutanenitrile (85%). This has to be ascribed to the characteristic surface properties of this catalyst which leads to a suficient coverage with weakly-bound hydrogen which permits the choice of lower reaction temperatures. At these lower temperatures, cyclization is not favoured and the amount of hydrogen available could produce monoamine selectively. If the reaction temperature is decreased and/or the hydrogen/adiponitrile ratio is decreased to a large extent, the monoamine selectivity increases.

REFERENCES

1. Weissermel, K., and Arpe, H.J., *"Industrial Organic Chemistry"*, Verlag Chemie, Berlin, 1978.
2. Volf, J., and Pasek, J., *"Catalytic Hydrogenation, Sudies in Surface Science and Catalysis"* (L.Cervený, Ed.), Vol. 27, Elsevier, Amsterdam, 1986.
3. Lazaris, A.Y., Zilberman, E.N., Lunicheva, E.V., and Vedin, A.M., *Zh. Prikl. Khim.* **38**, 1097 (1965).
4. Bolle, J., French Patent, FR2063378A1, 1971.
5. Medina, F., Salagre, P., Sueiras, J.E., and Fierro, J.L.G., *J. Mol. Catal.* **68**, L17 (1991).
6. Prins, R. *Catal. Today* **37**, 103 (1997).
7. Harrison., C.R., *"Catalysis and Chemical Processes"* (R.Pearce and W.R. Patterson, Eds), Chapter 7, 1981.
8. Mares, F., Galle, J.E., Diamond, S.E., and Regina, F. J., *J. Catal.* **112**, 145 (1988).
9. Huang, Y., and Sachtler, W. M. H., *Appl. Catal A: Gen.* **182**, 365 (1999).

10. Augustine, R.L., *Catal. Rev.* **13**, 285 (1976).

11. Frank, G., and Neubauer, G., German Patent DE3402734A1, 1984 (BASF AKTIENGESELLSCHAFT).

12. Greenfield, H., *Ind. Eng. Chem. Prod. Res. Develop*. **6**, 142 (1967).

13. Pasek, J., Kostova, N., and Dvorak, B., *Collect. Czech. Chem. Comunn*. **46**, 1011 (1981).

14. Schowoegler, E. J., and Adkins, H., *J. Am. Chem. Soc.* **61**, 3449 (1939).

15. Medina, F., Salagre, P., Sueiras, J. E., and Fierro, J.L.G., *Appl. Catal. A: Gen*. **92**, 131 (1992).

16. Medina, F., Salagre, P., Sueiras, J.E., and Fierro, J.L.G., *Solid State Ionics* **59**, 205 (1993).

17. Medina, F., Salagre, P., Sueiras, J.E., and Fierro, J.L.G., *Appl. Catal. A: Gen*. **99**, 115 (1993).

18. Medina, F., Salagre, P., Sueiras, J.E., and Fierro, J.L.G., *J. Chem. Soc. Faraday Trans.* **90**(10), 1455 (1994).

19. Medina, F., Dutartre, R., Tichit, D., Coq, B., Dung, N. T., Salagre, P., and Sueiras, J.E. *J. Mol Catal. A: Chem.* **119**, 201 (1997).

20. Dung, N.T., Tichit, D., Chiche, B.H., and Coq, B., *Appl. Catal. A: Gen.* **169**, 179 (1998).

21. Medina, F., Salagre, P., Sueiras, J. E., and Fierro, J.L.G., *J. Chem. Soc. Faraday* Trans. **89**(21), 3981 (1993).

22. Yu, X., Li, H., and Deng, J.F., *Appl. Catal. A: Gen.* **199**, 191 (2000).

23. M. Serra, P. Salagre, Y. Cesteros, F. Medina, J. E. Sueiras, *Solid State Ionics*, **134**, 229 (2000).

24. Estellé, J., Ph.D. thesis, Rovira i Virgili University, Tarragona, Spain, 1998.

25. Bish, D.L., and Howard, S.A., *J. Appl.Cryst.* **21**, 86 (1988).

26. Arena, F., Frusteri, F., Parmaliana, A., Plyasova, L., and Shmakov, A.N., *J. Chem. Soc., Faraday Trans.* **92**, 469 (1996).

27. Parmaliana, A., Arena, F., Frusteri, F., and Giordano, N., *J. Chem. Soc. Faraday Trans.* **86**(14), 2663 (1990).

28. Arena, F., Frusteri, F., and Parmaliana, A., *Appl. Catal A: Gen.* **187**, 127 (1999).

29. Anderson, P.J., and Hohrlock, R. F., *Trans.Faraday Soc.* **58**, 1993 (1962).

30. Páal, Z., and Menon, P.G., *Catal.Rev.-Sci.Eng.* **25**(2), 229 (1983).

31. Marcel Dekker *"Hydrogen Effects in Catalysis"*, (Paál, Z. and Menon, P.G., Eds.), New York, 1988.

32. Falconer, J.L., and Schwarz, J.A., *Catal. Rev.-Sci.Eng.* **25**, 141 (1983).

33. Raupp, G.B., and Dumesic, J.A., *J. Catal.* **95**, 587 (1985).

34. Raupp,G.B., and Dumesic, J.A., *J. Catal.* **97**, 85 (1986).

35. Arai, M., Nishiyama, Y., Masuda, T., and Hashimoto, K., *Appl. Surf. Sci.* **89**, 11 (1995).

36. Ferreira-Aparicio, P., Guerrero-Ruiz, A., and Rodriguez-Ramos, I., *J. Chem. Soc., Faraday Trans.* **93**(19), 3563 (1997).

37. Popova, N. M., Babenkova, L.V., and Sokol'skii, D.V., *Kinet. Katal.* **10**(5), 1177 (1969).

38. Bartholomew, C.H., *Catal. Lett.* **7**, 27 (1990).

39. Lee, P.I., and Schwartz, J.A., *J. Catal.* **73**, 272 (1982).

40. Zielinski, J., *Polish. J. Chem.* **69**, 1187 (1995).

41. Smeds, S., Salmi, T., Lindfors, L.P., and Krause, O., *Appl. Catal. A: Gen.* **144**, 177 (1996).

42. Kramer, P., and Andre, M., *J. Catal.* **58**, 287 (1979).

43. Konvalinka, J.A., Van Oeffelt, P.H., and Scholten, J.J.F., *Appl. Catal.* **1**, 141 (1981).

44. Weatherbee, G.D., and Bartholomew, C.H., *J. Catal.* **87**, 55 (1984).

45. Spinicci, R., and Tofanari, A., *React.Kinet.Catal.Lett.* **27**, 65 (1985).

46. Ikushima, Y., Arai, M., and Nishiyama, Y., *Appl. Catal.* **11**, 305 (1984).

47. Glugla, P.G., Bailey, K.M., and Falconer, J.L., *J. Catal.* **115**, 24 (1989).

48. Rankin, J.L., and Bartholomew, C.H. *J. Catal.* **100**, 533 (1986).

49. Stockwell, D.M., Bertucco, A., Coulston, GW., and Bennet, C.O., *J. Catal.* **113**, 317 (1988).

50. Cesteros, Y., Salagre, P., Medina, F., and Sueiras, J.E., *Appl. Catal. B: Environ.* **25**, 213 (2000).

51. Cesteros, Y., Salagre, P., Medina, F., and Sueiras, J.E., *Appl. Catal. B: Environ.* **22**, 135 (1999).

52. Marécot, P., Paraiso, E., Dumas, J.M., and Barbier, J., *Appl. Catal.* **74**, 261 (1991).

IV.2.2 Catalizadores de níquel-magnesia: una alternativa en la hidrogenación de 1,6-hexanodinitrilo.

Journal of Catalysis 209, páginas 202-209

doi:10.1006/jcat.2002.3617

Nickel-Magnesia Catalysts: an alternative for the hydrogenation of 1,6-Hexanedinitrile.

Marc Serra[a], Pilar Salagre[a*], Yolanda Cesteros[a], Francisco Medina[b] and Jesús E. Sueiras[b].

[a] *Facultat de Química, Universitat Rovira i Virgili, 1.43005, Tarragona, Spain.*

e-mail: salagre@quimica.urv.es

[b] Escola Tècnica Superior d'Enginyeria Química, Universitat Rovira i Virgili,

Av. Països Catalans, 26, 43007, Tarragona, Spain

ABSTRACT

Two Ni-MgO systems were synthesized and characterized in order to be studied as nickel catalysts for the hydrogenation of 1,6-hexanedinitrile (adiponitrile) in the gas phase. The activity results were compared with those obtained for a commercial Raney-Ni. All three catalysts showed high selectivities to 1,6-hexanediamine for a total conversion with a maximum of 96% for the Ni-MgO catalyst which has solid solution. However, only Ni-MgO catalysts showed a high selectivity to 6-aminohexanenitrile (83% and 77%, respectively) and a high conversion (87% and 85%, respectively). The higher selectivity to 6-aminohexanenitrile could be related with the presence of octahedral crystallites for Ni-MgO catalysts.

Key Words: Nickel-magnesia catalysts; magnesia; adiponitrile; dinitrile; 1,6- hexanedinitrile hydrogenation, 6-aminohexanenitrile, 1,6-hexanediamine.

INTRODUCTION

Catalytic hydrogenation of nitriles is an important industrial route for the manufacture of a great variety of amines [1-3], especially of 1,6-hexanediamine and 6-aminohexanenitrile. This is confirmed by several recent patents [4-15].

The hydrogenation of adiponitrile to 1,6-hexanediamine [16,17] is an interesting industrial process in the preparation of Nylon-6,6 and also to obtain 6-aminohexanenitrile [18,19], which is used in the preparation of caprolactam (precursor of Nylon-6) [20].

Caprolactam is mainly produced from cyclohexanone, a process that generates 4.5 Kg of ammonium sulfate per kg of caprolactam produced. However, Rhodia is developing a new salt-free process to obtain caprolactam with lower costs than the current process. The first step of this new process is the hemihydrogenation of 1,6-hexanedinitrile (adiponitrile) to 6-aminohexanenitrile. [21].

This allows to minimize wastes, one of the arguments of the green chemistry for the manufacture and application of chemical products [22].

The main products of nitriles hydrogenation are usually mixtures of amines [23,24]. The condensation reactions between a highly reactive intermediate imine and the primary amine always lead to the formation of products such as secondary and tertiary amines together with the primary amine [25]. Catalysts based on Co, Ni, and Ru are mostly used to produce primary amines [6,7,13,14, 18, 26-29].

The addition of potassium in small amounts enhances as well the selectivity of nickel catalysts towards primary amines in the adiponitrile hydrogenation [30-33]. Other precursors, such as hydrotalcites of Ni/Mg/Al, allow to vary the MgO/Al_2O_3 ratio and, thus, control the acidity of the final catalysts [34,35]. When this ratio increases, the selectivity to primary amines increases for the hydrogenation of acetonitrile.

From studies of the preparation conditions of NiO-MgO systems, it is assumed that the reducibility of the corresponding NiO phase and the final properties of the nickel phase (size, morphology...) are highly affected by the tendency to form solid solutions of NiO-MgO [36-39].

Additionally, Ni/MgO catalytic systems have shown a considerable inhibitory effect on the generation of graphitic residues in several reactions [40].

In previous work [41], Ni-MgO systems showed high activity for the hydrogenation of 1,4-butanedinitrile with a highest selectivity to 4-aminobutanenitrile of 85 %. We also reported that the crystal morphology could induce certain selectivity to the monoamine [42-45]. However, the recent literature about the hemihydrogenation of adiponitrile [4,15, 17-19, 46-48] shows still difficulties to achieve selective hydrogenation with high conversion.

Our goal is to obtain nickel systems that can catalyze the hydrogenation of 1,6-hexanedinitrile, and control the selectivity to 6-aminohexanenitrile and 1,6-hexanediamine.

Therefore, two Ni-MgO catalysts are prepared and tested for the hydrogenation of adiponitrile. Their catalytic results will be compared with those obtained for an usual industrial hydrogenation catalyst: Raney-Ni [7,13].

EXPERIMENTAL

Catalysts preparation

Two NiO/MgO systems were prepared, with a weight ratio of 4:1 (referred to as 4), and a commercial MgO_{C3} (Aldrich, 99%, BET area of 21 m^2g^{-1}, referred to as C_3) as the MgO source.

Sample $4C_3B$ was prepared by thermal decomposition of a $Ni(NO_3)_2{\cdot}6H_2O$ and MgO mixture and subsequent calcination under static air according to the method previously described [41].

Sample $4C_3C$ was prepared by means of controlled thermolysis of $Ni(NO_3)_2{\cdot}6H_2O$ at 373 K for 14 days to obtain $Ni_3(NO_3)_2(OH)_4$, which was then mixed with MgO. This mixture was subsequent calcined at 523 K under an argon flow.

The Raney-nickel was a commercial nickel sponge suspension in water (Fluka 99%) and was dried under H_2 flow at 453 K for 1 h (referred to as Raney-Ni). The NiO-MgO systems ($4C_3B$ and $4C_3C$) were reduced under pure H_2 at 673 K for 6 h (catalysts $R4C_3B$ and $R4C_3C$, respectively). The catalysts, after the catalytic reaction, are named as Raney-Ni_{AC}, $R4C_3B_{AC}$, and $R4C_3C_{AC}$.

Characterization methods

BET surface areas were calculated from the nitrogen adsorption isotherms at 77 K using a Micromeritics ASAP 2000 surface analyser and a value of 0.164 nm^2 for the cross-section of the nitrogen molecule.

Powder X-ray diffraction patterns of the samples were obtained with a Siemens D5000 diffractometer using nickel-filtered Cu Kα radiation. This technique was also used to determine the reduction degree (α) of the catalysts by means of the Rietveld method [49].

Temperature-programmed reduction studies (TPR) were carried out in a Labsys/Setaram TG DTA/DSC, equipped with a 273-1273 K programmable temperature furnace. Each sample was first heated at 423 K in an Ar flow until no change of weight was detected. Then, the sample was heated in a 5vol% H_2/Ar flow from 423 K to 1173 K at a rate of 5 K min^{-1}.

Hydrogen chemisorption was measured with a Micromeritics ASAP 2010C equipped with a turbomolecular pump. Samples had been previously reduced under the same conditions as for preparing the catalysts and the hydrogen was analysed at 303 K. Coenen in chemisorption studies of nickel catalysts, pointed out the importance to employ a long equilibration time [50]. A longer equilibration interval improves the data integrity and consequently, a higher chemisorption is obtained due to the slow equilibrium kinetics of hydrogen. In order to obtain the optimum amount of chemisorbed hydrogen for each catalyst, the equilibration intervals were increased until no different metallic area values were obtained. The nickel surface area was

calculated assuming a stoichiometry of one hydrogen molecule per two surface nickel atoms and an atomic cross-sectional area of 6.49×10^{-20} m^2/Ni atom.

Temperature-programmed desorption (TPD) were obtained with a FISONS QTMD 150 gas desorption unit equipped with a 273-1273 K programmable temperature furnace and a mass spectrometer detector. Samples had been previously reduced under the same conditions as for preparing the catalysts. The desorption carried out from room temperature to 1123K with a rate of 10 K min^{-1}.

Scanning electron micrographs (SEM), were obtained with a JEOL JSM6400 scanning microscope operating at an accelerating voltage in the range 30-35 kV.

Determination of the catalytic activity

The gas phase hydrogenation of 1,6-hexanedinitrile at atmospheric pressure (1 torr) was studied in a tubular fixed-bed flow reactor heated by an oven equipped with a temperature control system. The reactor was filled with catalyst (500 mg of precursors $4C_3B$, $4C_3C$ and 314 mg of Raney-Ni).

Reaction products were analysed by an on-line gas-chromatograph HP 5890 equipped with a 30 m “commercial Rtx-5 amine” cappillary column and a flame ionization detector.

RESULTS AND DISCUSSION

Characterization of the catalyst precursors

Table 1 shows characterization data of the catalyst precursors. Sample $4C_3B$ shows diffraction lines which can be identified as NiO-MgO solid solution phase [39, 41]. In contrast, sample $4C_3C$ only has diffraction peaks of the NiO phase.

The use of an argon flow through the sample during calcination could make the diffusion between the NiO and MgO phases for sample $4C_3C$ difficult. This is in agreement with Arena et al. who reported the importance of diffusion on the formation of a solid solution [36, 37].

TABLE 1

Characterization of the catalytic precursors

	$4C_3B$	$4C_3C$
Crystalline phases (XRD)	NiO-MgO	NiO
Crystallite sizes (nm) [a]	35.2	16.1
T_R (K) (TPR) [b]	604	523
Surface area (m^2g^{-1})[c]	36.8	86.9

[a] Using Scherrer equation.
[b] T_R = initial reduction temperature, obtained by TPR experiments.
[c] Using BET area method.

The reducibility of the two NiO-MgO systems was estimated by TPR by comparing their initial reduction temperature values (T_R). The initial reduction temperature of sample $4C_3C$ is considerably lower than that of sample $4C_3B$ (Table 1). This confirms the low interaction between the NiO and MgO phases for sample $4C_3C$.

The higher initial reduction temperature of sample $4C_3B$ is in agreement with the results of Arena and Parmaliana et al. [36-38] and more recent studies [39,41], which reported that the formation of a solid solution hinders the reduction of NiO.

Also, Ruckenstein and Hang Hu reported that the electronic transfer between NiO and MgO involves strong interactions, which inhibit the reduction of NiO [51].

The surface area of the NiO-MgO systems is 36.8 m^2g^{-1} for $4C_3B$, and 86.9 m^2g^{-1} for $4C_3C$ (Table 1). The higher surface area of the catalytic precursor $4C_3C$ than of $4C_3B$ could be due to the use of an argon flow. This favors the efficient elimination of decomposition products and, therefore, the agglomeration effect is lower.

The morphology and particle size for the different precursors of NiO-MgO has been observed by SEM. Samples $4C_3B$ and $4C_3C$ shows octahedral particles around 100-300 and 50-150 nm, respectively. The values observed are in agreement with the BET area results.

Characterization of the catalysts before reaction

Table 2 shows the crystalline phases obtained by XRD for the three catalysts and the reduction degree (α) at the given reduction conditions. The Raney-Ni and B catalysts have crystalline nickel as single phase and show total reduction (α=1).

However, catalyst A shows a powder diffraction pattern corresponding to two phases: a crystalline solid solution phase and a less crystalline Ni phase. The partial reduction obtained for catalyst A

(α=0.71) is in agreement with the lower reducibility of its precursor as observed by TPR.

After reduction, catalyst R4C_3C exhibits a lower surface area (20.5 m^2g^{-1}) than its catalytic precursor (86.9 m^2g^{-1}). This decrease could be related to the fast reduction observed for this catalyst, which facilitates a higher agglomeration of metallic particles.

TABLE 2
Characterization of the catalysts before reaction.

	Raney-Ni	R4C_3B	R4C_3C
Crystalline phases (XRD)	Ni	Ni NiO-MgO	Ni
Crystallite sizes of Ni (nm)[a]	9.2	9.2	62.6
Surface area (m^2g^{-1})[b]	72.8	42.3	20.5
Metallic area (m^2g^{-1} catalyst)[c]	31.0	16.1	2.0
Reduction degree α[d]	1	0.71	1

[a] Using Scherrer equation
[b] Using BET area method.
[c] Metal surface area, calculated from chemisorbed H_2.

On the other hand, there are only slight differences in the BET area values for the precursor 4C_3B (36.8 m^2g^{-1}) and its corresponding catalyst R4C_3B (42.3 m^2g^{-1}). This is in agreement with the better dispersion of NiO observed when the precursor is a solid solution. In that case, the reduction is slow and the sintering effect will be smaller, as confirmed by its crystallite size (Table 2).

The surface area of the commercial Raney-Ni catalyst after drying at 453 K was high (72.8 m^2g^{-1}), as was expected from to the sponge structure of this nickel.

Table 2 also shows the results of H_2 adsorption experiments. The Raney-Ni catalyst has a higher metallic area (31.0 m^2g^{-1}catalyst) than catalyst $R4C_3B$ (16.1 m^2g^{-1}catalyst) and catalyst $R4C_3C$ (2.0 m^2g^{-1}catalyst). These values are in agreement with their nickel crystallite sizes.

The difference between the two catalysts prepared with magnesia could be again related to a higher sintering effect produced during the reduction step for the sample that has not formed a solid solution. Therefore, catalyst $R4C_3C$ has a higher crystallite size and lower BET and metallic area values than catalyst $R4C_3B$.

The TPD hydrogen studies show some differences between the three catalysts. The Raney-Ni catalyst shows two hydrogen desorption peaks clearly differentiated with similar intensity and with maxima at 427 K and 505 K (Fig. 1). In contrast, catalyst $R4C_3B$ only shows one hydrogen desorption peak with a maximum at 446 K and catalyst $R4C_3C$ shows three maximum of hydrogen desorption at 405, 513, and 606 K.

Interestingly, the TPD spectrum of catalyst $R4C_3C$ is similar to the TPD spectrum reported in a previous work for a bulk nickel catalyst, with octahedral crystals, which was obtained from decomposition of nickel nitrate (41). The difference is just a slight shift to lower temperatures for catalyst $R4C_3C$. This catalyst also has a low metallic area, as the bulk nickel catalyst. These similarities are probably related to the fact that catalyst $R4C_3C$ does not form a solid solution.

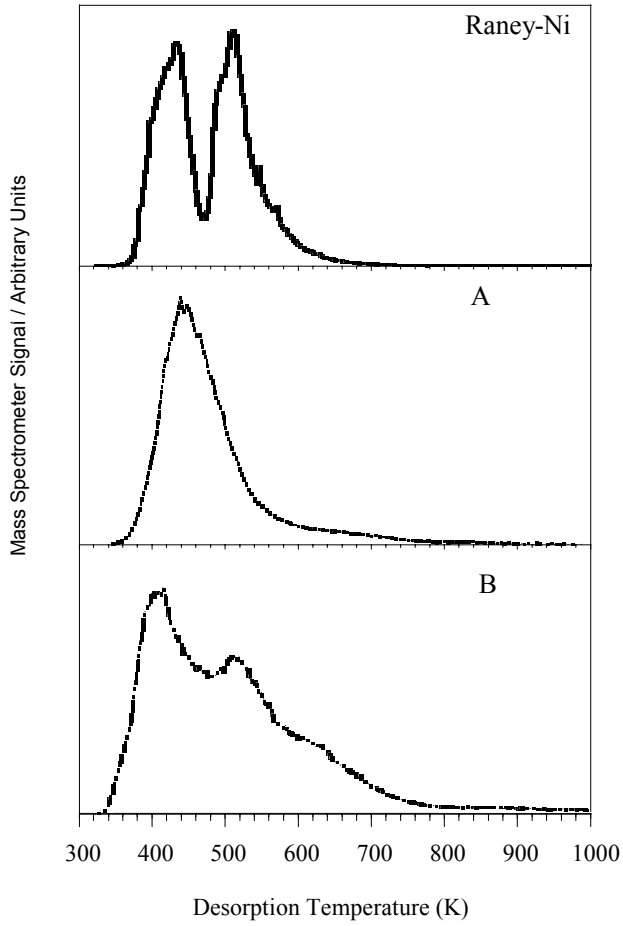

Fig. 1. H_2 TPD plots for the three catalysts.

The SEM micrograph of catalyst R4C$_3$B does not show significant differences in size and morphology with respect to its catalytic precursor. However, in the micrograph of catalyst R4C$_3$C a partial agglomeration of particles was observed when compared with its catalytic precursor.

Characterization of the catalysts after catalytic reaction.

Table 3 shows the characterization of the catalysts after reaction. Catalysts $R4C_3B_{AC}$ and Raney-Ni_{AC} almost have the same nickel crystallite size (around 10 nm) as before catalysis. However, the surface areas (15.6 and 22.3 m^2g^{-1}) and metallic areas (2.5 and 4.2 m^2g^{-1}catalyst) have decreased for both catalysts ($R4C_3B_{AC,}$ and Raney-Ni_{AC}, respectively). Finally, there is a slight decrease of metallic particle size (49.9 nm) together with a small increase of the surface area (26.5 m^2g^{-1}), but the metallic area decreases slightly (1.6 m^2g^{-1}catalyst) for catalyst $R4C_3C_{AC.}$

TABLE 3

Characterization of the catalysts after reaction

	Raney-Ni_{AC}	$R4C_3B_{AC}$	$R4C_3C_{AC}$
Crystalline phases (XRD)	Ni	Ni NiO-MgO	Ni
Crystallite sizes of Ni (nm)[a]	10.5	10.9	49.9
Surface area (m^2g^{-1})[b]	22.3	15.6	26.5
Metallic area (m^2g^{-1} catalyst)[c]	4.2	2.5	1.6

[a] Using Scherrer equation.
[b] Using BET area method.
[c] Metal surface area, calculated from chemisorbed H_2.

The results obtained for catalysts $R4C_3B_{AC}$ and Raney-Ni_{AC} cannot be explained by the sintering of this nickel metallic phase because its crystallite size is maintained. The formation of small

amounts of high-molecular-weight products at the reaction conditions tested can probably produce a partial coverage or decoration of the Ni particles, which could be responsible for the decrease of the surface area and metallic area.

On the other hand, the surface modifications observed in catalyst $R4C_3C_{AC}$ could be related to two simultaneous effects: 1) a small disagglomeration of Ni and MgO particles during reaction, 2) a decoration, mainly of Ni particles, with the condensation products.

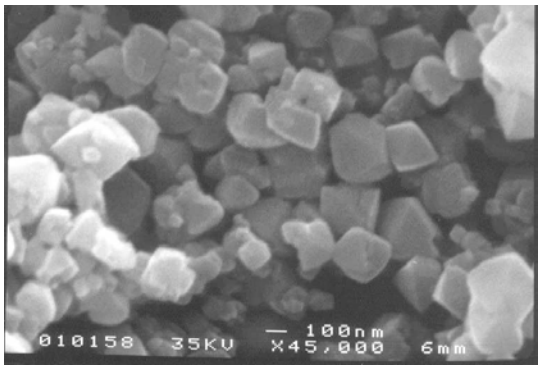

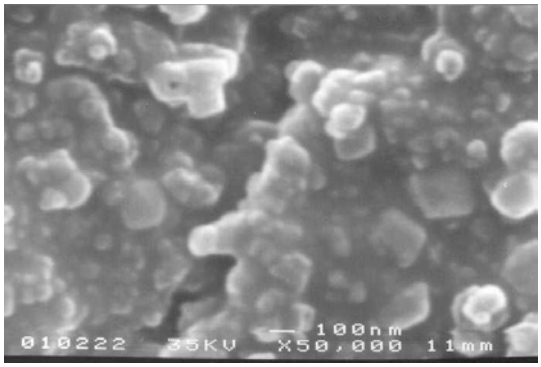

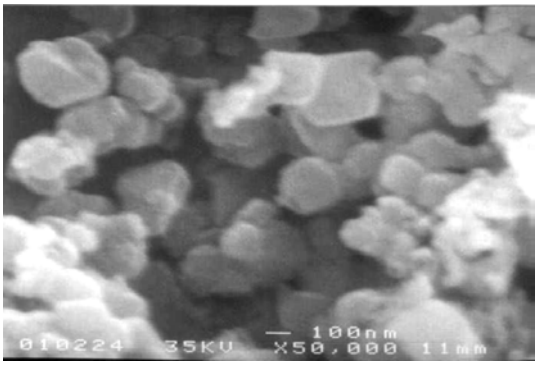

Fig. 2. Scanning electron micrographs of: a) catalyst $R4C_3B_{AC}$, b) catalyst $R4C_3C$ and c) catalyst $R4C_3C_{AC}$.

Fig. 2. a, b, and c show the SEM micrographs of catalyst $R4C_3B_{AC}$, B $R4C_3C$ and $R4C_3C_{AC}$, respectively. After reaction, catalyst $R4C_3B$ shows similar sizes and octahedral morphologies as before reaction. However, for catalyst $R4C_3C$, particles are better defined after reaction than before.

Catalytic Activity

Tables 4 and 5 show conversions and selectivities for the hydrogenation of 1,6-hexanedinitrile on nickel and nickel-magnesia catalysts (catalysts Raney-Ni, $R4C_3B$, and $R4C_3C$) under the conditions given in the Experimental section.

The comparison of the catalytic activity of these catalysts was carried out at the same H_2/ADN ratios and at the same theoretical amount of Ni as active phase.

Taking into account that the selectivity towards the different reaction products could be related to the reaction conditions [41], the

comparative study has been performed at different reaction temperatures, space velocities, and H_2/ADN molar ratios.

In order to have the same H_2/ADN ratios for the three catalysts, the space velocities for the Raney-Ni catalyst were higher. The catalytic results for each catalyst are given in four groups of conditions: a) ratio H_2/ADN = 6738, reaction temperature = 363 K; b) H_2/ADN = 1002, reaction temperature = 383 K; c) H_2/ADN = 178, reaction temperature = 423 K and d) H_2/ADN =9, reaction temperature = 473 K. In addition, some results at lower H_2/ADN ratios at the same reaction temperature are also included for the Raney-Ni catalyst (Table 4).

TABLE 4
Catalytic behavior of the Raney-Ni catalyst for the hydrogenation of 1,6-hexanedinitrile.

Catalyst	H_2/ADN ratio	Space velocity (h^{-1})	Reaction temp. (K)	Conversion (%)	Selectivity %					
					1-Azacyclo heptane HHAPN	3,4,5,6-Tetrahydro-2H-azepine THAPN	6-Aminohexane nitrile AHN	1,6-Hexane diamine HMA	Cracking Products	Condensation products
Raney-Ni	6738	71620	363	100	0	0	14	86	0	0
	1002	47747	383	80	8	3	60	29	0	0
	1002	34139	383	95	18	12	33	37	0	0
	178	23873	423	100	45	0	0	36	11	8
	178	71620	423	99	16	0	8	67	8	1
	59	71620	423	64	14	4	33	32	15	2
	9	23873	473	90	22	5	28	34	8	3
	9	5968	473	100	53	0	0	17	25	5
	4	5968	473	97	23	5	23	37	12	0

TABLE 5
Catalytic behavior of Ni-MgO catalysts for the hydrogenation of 1,6-hexanedinitrile.

Catalyst	H_2/ADN ratio	Space velocity (h^{-1})	Reaction temp. (K)	Conversion (%)	Selectivity %					
					1-Azacycloheptane HHAPN	3,4,5,6-Tetrahydro-2H-azepine THAPN	6-Aminohexane nitrile AHN	1,6-Hexane diamine HMA	Cracking Products	Condensation products
R4C$_3$B	6738	21486	363	100	0	0	3	96	0	1
	1002	10242	383	87	0	1	83	16	0	0
	178	1790	423	100	60	0	0	28	5	7
	178	7162	423	55	0	0	87	7	0	6
	9	895	473	93	44	2	1	5	48	0
	9	14324	473	65	4	0	65	12	15	4
R4C$_3$C	738	21486	363	100	12	0	1	84	0	0
	1002	10242	383	85	23	0	77	0	0	0
	178	1790	423	100	18	2	49	22	0	9
	178	7162	423	30	2	2	81	8	1	6
	9	895	473	93	28	1	16	46	6	3
	9	14324	473	56	3	1	77	15	1	3

By-products such as condensation compounds, which are dimers produced by an intermolecular amine-imine condensation reaction, were obtained in small amounts (0-9%) for all catalysts. For catalysts $R4C_3B$ and $R4C_3C$, this is probably due to the basic character of magnesia, which favors the elimination of amines and prevents secondary reactions. These results are in agreement with those previously reported for the hydrogenation of 1,4-butanedinitrile (41). However, the Raney-Ni behavior could be related to its high activity, which favors the fast hydrogenation of the imine intermediate in front of the condensation reactions. Moreover, the Raney-Ni and $R4C_3B$ catalysts show the highest amount of cracking products (Table 4 and 5) which can be related to their higher metallic areas.

The reaction mechanisms proposed in the literature for the hydrogenation of dinitriles show different reaction products of partial and total hydrogenation [23]. This mechanism together with the results reported in recent studies for the hydrogenation of acetonitrile [52], 1,4-butanedinitrile [41] and 1,6-hexanedinitrile [42-45], and also with the results presented in this work, allows us to propose a sequence of the main catalytic hydrogenation products of 1,6-hexanedinitrile (Scheme 1).

This scheme shows that the formation of different products is directly related to the consume of different hydrogen amounts and to the hydrogenation rate of each step. Consequently, the selectivity could be controlled by means of the active hydrogen available (different for each catalyst and depending on the temperature reaction) and the contact time. The presence of cracking and cyclic products is probably related to more active systems (high hydrogen amounts available). The cyclic compound (HHAPN) needs the same theoretical hydrogen consumption as the diamine (HMA) but has a slower rate of formation

and higher thermodynamic stability. Consequently, the production of HHAPN is favored at higher hydrogen amounts.

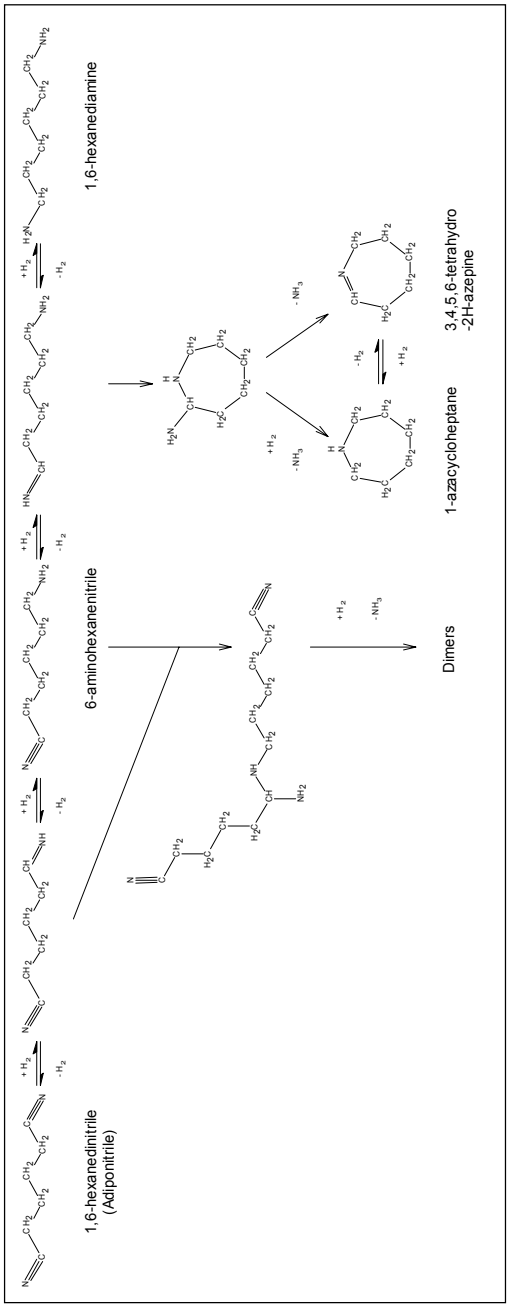

Scheme 1. Possible products obtained by catalytic hydrogenation of 1,6-hexanedinitrile (adiponitrile).

The results in Tables 4 and 5 show that the Raney-Ni catalyst is more active than the systems with magnesia at all reaction temperatures tested for the same H_2/ADN ratios (higher conversions, higher amounts of cyclic and cracking products at higher space velocity). At lower temperatures, the activity differences of Raney-Ni catalyst with the Ni-MgO catalysts decrease.

At reaction temperatures above 423 K, catalyst R4C_3B is slightly more active than catalyst B (higher amounts of HHAPN). However, catalyst R4C_3C seems slightly more active than catalyst R4C_3B below to 423 K (higher amounts of HHAPN). Actually, taking into account the metallic area and TPD results, small differences could be expected. There are great differences in the metallic area values between the three catalysts before reaction, but, after reaction, these differences decrease considerably (Tables 2 and 3).

Some authors correlated the binding strength of the chemisorbed hydrogen with the activity for a specific reaction [53-56]. In our experiments the activity for each catalyst could be related with its hydrogen TPD values. Catalyst R4C_3C has the lowest metallic area but its hydrogen desorption starts before that of the other catalysts (405 K). This could explain its higher activity at lower temperatures.

The higher activity observed for catalyst R4C_3B at higher reaction temperatures could also be explained by its metallic area and its maximum hydrogen desorption at 446 K.

Formation of 1,6-hexanediamine

All catalysts show high selectivity towards 1,6-hexanediamine with values of 86% for the Raney-Ni catalyst and 84% for catalyst $R4C_3C$ as total conversion. Catalyst $R4C_3B$ shows the highest selectivity to 1,6-hexanediamine (96%) also as total conversion and at the same reaction conditions (363 K and H_2/ADN=6738) as the other catalysts.

In Scheme 1 we can see that cyclization products can compete with diamine when the hydrogen amount increases. However, in Tables 4 and 5 we observe that at lower temperature and higher space velocity, the diamine formation is favored. This is in agreement with the results reported in a previous [41].

The small differences observed between the three catalysts could be related to similar amounts of hydrogen available at lower temperature (Fig. 1). The second product obtained was 1-azacycloheptane (12%) for catalyst $R4C_3C$. However, catalyst $R4C_3B$, with only one hydrogen desorption peak (maximum at 446 K), has an insufficient amount of hydrogen to produce the slow cyclization reaction at lower reaction temperatures, and therefore, 1-azacycloheptane is not observed. The higher space velocity used for Raney-Ni (71620 h^{-1}) as for the others (21486 h^{-1}), explains the formation of 6-aminohexanenitrile (14%) for this catalyst.

We can conclude that the formation of 1,6-hexanediamine with these nickel catalysts is favored at high H_2/ADN ratios and at lower reaction temperatures since higher reaction temperatures lead to cyclization (1-azacycloheptane) and cracking products.

Formation of 6-aminohexanenitrile

Scheme 1 shows that the production of 6-aminohexanenitrile demands the lowest hydrogen consumption. In a previous work about the catalytic hydrogenation of 1,4-butanedinitrile with nickel-magnesia catalysts [41], we reported that when using low reaction temperatures, the amount of hydrogen available for these catalysts decreases, and consequently, the formation of the less hydrogenated species (4-aminobutanenitrile) increases. However, there are others parameters that influence the hydrogen consumption (ADN amounts, hydrogen flow, and contact time).

In order to obtain a high activity and selectivity to monoamine at different reaction temperatures, three different strategies have been proposed:

A) Reaction temperature at 383 K: low ADN vapor pressure (0.38 torr), medium values of H_2/ADN ratio (1002) and space velocity of 10242 h^{-1} have been used. Besides, higher space velocities have been used (47747, 34139 h^{-1}) for Raney-Ni catalyst.

A low vapor pressure gives rise to small amounts of adiponitrile passing through the reactor. This, together with the reaction parameters, leads to higher conversions (between 80 and 95%) for all catalysts. Catalysts R4C_3B and R4C_3C show high selectivities to 6-aminohexanenitrile (83% and 77%). In contrast, the best result for the Raney-Ni catalyst is slightly lower, 60% of monamine for 80% of conversion at the higher space velocity of 47747 h^{-1}. When decreasing the space velocity (34139 h^{-1}) the conversion increases (up to 95 %) but the selectivity to 6-aminohexanenitrile decreases to 33 %, as expected.

B) Reaction temperature at 423 K: moderate vapor pressure (4.28 torr), moderate H_2/ADN ratios (178). These conditions allow to considerably decrease the hydrogen amount. However, an increase of the contact time was necessary to not decrease the conversion for catalysts R4C$_3$B and R4C$_3$C too much (space velocity of 7162 h^{-1}). For the Raney-Ni catalysts, higher space velocities were tested (23873, 71620h^{-1}).

Again, catalysts R4C$_3$B and R4C$_3$C present a high selectivity to monoamine (87% and 81%, respectively). However, their conversions are lower (55% and 30%, respectively) than when using strategy R4C$_3$B. The Raney-Ni catalyst has very low selectivity to monoamine (8% at 71620 h^{-1} and 0% at 23873 h^{-1}) for a total conversion.

In order to improve the monoamine selectivity for the Raney-Ni catalyst, another reaction condition has been tested: a lower ratio H_2/ADN (59) at the highest space velocity (71620 h^{-1}). There is a slight increase in the selectivity to 6-aminohexanenitrile (33%) but the conversion is lower (64%).

C) Reaction temperature at 473 K: high vapor pressure (98.6 torr) of adiponitrile, low H_2/ADN ratio (9) and a space velocity of 14324 h^{-1} for catalysts R4C$_3$B and R4C$_3$C have been used. Under these conditions, the small hydrogen amount and the low contact time of adiponitrile in the reactor counteract the effect of the high reaction temperature. For the Raney-Ni catalyst, a higher space velocity has been tested (23873 h^{-1}).

Catalysts R4C$_3$B and R4C$_3$C show high selectivity to monoamine (65% and 77%, respectively). However, the conversions are lower than when using strategy A (65% and 56%, respectively). Also, under these

conditions, the Raney-Ni catalyst shows a lower selectivity to monoamine (28%) for a 90% of conversion.

In order to have more information about the catalytic behaviour of Raney-Ni, other reaction conditions have been tested: space velocity of 5968 h^{-1} for 9 and 4 H_2/ADN ratios. Now, by decreasing the H_2/ADN ratio, the selectivity to monoamine increases from 0 to 23 % for a similar conversion.

Independently of the reaction conditions used, the catalysts with magnesia present high selectivities to 6-aminohexanenitrile. However, not all the strategies designed for Raney-Ni catalyst allowed to obtain a high selectivity to the monoamine.

From these results, we can assume that the reaction conditions play an important role controlling the selectivity for the hydrogenation of 1,6-hexanedinitrile. Besides, the difference observed between the Ni-MgO and Raney-Ni catalysts could also be explained taking into account the effect of the particles morphology on the selectivity to 6-aminohexanenitrile.

In previous studies [41, 42-45], we reported that octahedral crystal sites could induce a certain selectivity to monoamine compounds. The results presented in this work support this approach since catalysts R4C_3B and R4C_3C, which present the higher selectivity to 6-aminohexanenitrile, show a considerable number of octahedral crystallites.

CONCLUSIONS

Two different nickel-magnesia catalysts have been prepared by two different paths and compared with a commercial Raney-Ni catalyst for the hydrogenation of 1,6-hexanedinitrile (adiponitrile).

All catalysts showed a high selectivity to 1,6-hexanediamine for a total conversion at 363 K with a maximum of 96% for catalyst R4C_3B, which is the Ni-MgO catalyst which has solid solution phase. This similar behaviour can be related to the similar amounts of hydrogen available at lower reaction temperatures for the three catalysts.

The Ni-MgO catalysts showed a higher selectivity to the 6-aminohexanenitrile than did Raney-Ni at all conditions tested. It is possible to obtain a high selectivity to the monoamine at different reaction conditions for catalysts R4C_3B and R4C_3C. A decrease of some reaction parameters (reaction temperature, H_2/ADN ratio, and contact time) favors the partial hydrogenation.

Catalysts R4C_3B and R4C_3C showed the highest selectivity to 6-aminohexanenitrile (83% and 77%, respectively) with higher conversions (87% and 85%, respectively) at 383 K, H_2/ADN of 1002 ratio and a of space velocity 10242 h^{-1}. The high selectivity to 6-aminohexanenitrile could also be related to the presence of octahedral crystallites, which could induce a selectivity to monoamine for catalyst R4C_3B and R4C_3C.

These preliminary studies make as believe that these Ni-MgO catalysts are suitable for the industrial manufacture of 1,6-

hexanediamine and 6-aminohexanenitrile with high selectivity and conversion. However, information about lifetime at the different reaction conditions is needed.

REFERENCES

53. Weissermel, K., and Arpe, H.J., *"Industrial Organic Chemistry",* Verlag Chemie, Berlin, 1978.

54. Volf, J., and Pasek, J., *"Catalytic Hydrogenation, Sudies in Surface Science and Catalysis"* (L.Cerveny Ed.), Vol. 27. Elsevier, Amsterdam, 1986.

55. Prins, R., *Catal. Today,* **37,** 103 (1997).

56. Vandenbooren, F., Bosman, H., and Van der Spoel, J., WIPO Patent WO9426699A1, 1994 (DSM N.V.).

57. Cordier, G., Fouilloux, P., Laurain, N., and Spindler, J.F., WIPO Patent WO9518090A1, 1995 (Rhone Poulenc Chimie).

58. Schnurr, W., Voit, G., Flick, K., Melder, J. P., Fischer, R., and Harder, W., WIPO Patent WO9737964A1, 1997 (BASF AKTIENGESELLSCHAFT).

59. Koch, T. A., Krause, K. R., and Sengupta, S. K., WIPO Patent WO9843940A1, 1998 (E.I. DuPont de Nemours and Company).

60. Leconte P., WIPO Patent WO9959962A1, 1998 (Rhodia Fiber and Resin Intermediates).

61. Boschat, V., Leconte, P., Rochette, D., and Sever, L., WIPO Patent WO9926917A1, 1999 (Rhodia Fiber and Resin Intermediates).

62. Luyken, H., Ohbach, F., Ansmann, A., Bassler, P., Fischer, R., Melder, J. P., Merger, M., Rehfinger, A., Voit, G., and Achhammer, G., WIPO Patent WO005191A1, 2000 (BASF AKTIENGESELLSCHAFT).

63. Luyken, H., Ohbach, F., Ansmann, A., Bassler, P., Fischer, R., Melder, J. P., Merger, M., Rehfinger, A., Voit, G., and Achhammer, G., WIPO Patent WO012459A1, 2000 (BASF AKTIENGESELLSCHAFT).

64. Fischer, R., Bassler, P., Luyken, H., Ohbach, F., Melder, J. P., Merger, M., Ansmann, A., Rehfinger, A., and Voit, G., WIPO Patent WO012460A1, 2000 (BASF AKTIENGESELLSCHAFT).

65. Boschat, V., and Brunelle, J. P., WIPO Patent WO027806A1, 2000 (Rhodia Fiber and Resin Intermediates).

66. Harper, M. J., WIPO Patent WO027526A1, 2000 (E.I. DuPont de Nemours and Company).

67. Ionkin, A. S., Ziemecki, S. B., Koch, T. A., and Bryndza, H. E., WIPO Patent WO064862A3, 2000.

68. Lazaris, A.Y., Zilberman, E.N., Lunicheva, E.V., and Vedin, A.M., *Zh. Prikl. Khim.* **38**, 1097 (1965).

69. Medina, F., Salagre, P., Sueiras, J.E., and Fierro, J.L.G., *J. Mol. Catal.* **68**, L17 (1991).

70. Diamond, S.E., Mares F., and Szalkiewicz, A., EPO Patent EP077911A1, 1983 (Allied Corporation).

71. Sanchez, K. M., EPO Patent EP642493B1, 1996 (E. I. DuPont Nemours and Company).

72. Brunelle, J. P., Seigneurin, A., and Sever, L., WIPO Patent WO005203A1, 2000 (Rhodia Fiber and Resin Intermediates).

73. Sheldon, R., *Green Chem.* **2**(1), G1 (2000).

74. Clark, J., *Green Chem.* **1**(1), 1 (2000).

75. Mares, F., Galle, J.E., Diamond, S.E., and Regina, F. J., *J. Catal.* **112**, 145 (1988).

76. Huang, Y., and Sachtler, W. M. H., *Appl. Catal A: Gen.* **182**, 365 (1999).

77. Augustine, R.L., *Catal. Rev.* **13**, 285 (1976).

78. Frank, G., and Neubauer, G., Germany Patent DE3402734A1, 1984 (BASF AKTIENGESELLSCHAFT).

79. Greenfield, H., *Ind. Eng. Chem. Prod. Res. Develop*. **6**, 142 (1967).

80. Pasek, J., Kostova, N., and Dvorak, B., *Collect. Czech. Chem. Comunn*. **46**, 1011 (1981).

81. Schowoegler, E. J., and Adkins, H., *J. Am. Chem. Soc.* **61**, 3449 (1939).

82. Medina, F., Salagre, P., Sueiras, J. E., and Fierro, J.L.G., *Appl. Catal. A: Gen*. **92**, 131 (1992).

83. Medina, F., Salagre, P., Sueiras, J.E., and Fierro, J.L.G., *Solid State Ionics* **59**, 205 (1993).

84. Medina, F., Salagre, P., Sueiras, J.E., and Fierro, J.L.G., *Appl. Catal. A: Gen*. **99**, 115 (1993).

85. Medina, F., Salagre, P., Sueiras, J.E., and Fierro, J.L.G., *J. Chem. Soc. Faraday Trans*. **90**(10), 1455 (1994).

86. Medina, F., Dutartre, R., Tichit, D., Coq, B., Dung, N. T., Salagre, P., and Sueiras, J.E. *J. Mol Catal. A: Chem.* **119**, 201 (1997).

87. Dung, N.T., Tichit, D., Chiche, B.H., and Coq, B., *Appl. Catal. A: Gen.* **169**, 179 (1998).

88. Parmaliana, A., Arena, F., Frusteri, F., and Giordano, N., *J. Chem. Soc. Faraday Trans.* **86**(14)**,** 2663 (1990).

89. Arena, F., Frusteri, F., Parmaliana, A., Plyasova, L., and Shmakov, A.N., *J. Chem. Soc., Faraday Trans.* **92**, 469 (1996).

90. Arena, F., Frusteri, F., and Parmaliana, A., *Appl. Catal A: Gen.* **187**, 127 (1999).

91. Serra, M., Salagre, P., Cesteros, Y., Medina, F., and Sueiras, J.E., *Solid State Ionics* **134**, 229 (2000).

92. Bhattacharyya, A., and Chang, W.W., "*Catalyst Deactivation, Studies in Surface Science and Catalysis* " (Delmon, B., and Froment, G. F., Ed.), Vol. 88. Elsevier, Amsterdam, 1994

93. Serra, M., Salagre, P., Cesteros, Y., Medina, F., and Sueiras, J.E., *J. Catal.* **197**, 210 (2001).

94. Medina, F., Salagre, P., Sueiras, J. E., and Fierro, J.L.G., *J. Catal.* **142**, 392 (1993).

95. Medina, F., Salagre, P., Sueiras, J. E., and Fierro, J.L.G., *J. Mol. Catal.* **81**, 363 (1993).

96. Medina, F., Salagre, P., Sueiras, J. E., and Fierro, J.L.G., *J. Chem. Soc. Faraday* Trans. **89**(18), 3507 (1993).

97. Medina, F., Salagre, P., Sueiras, J. E., and Fierro, J.L.G., *J. Chem. Soc. Faraday* Trans. **89**(21), 3981 (1993).

98. Yu, X., Li, H., and Deng, J.F., *Appl. Catal. A: Gen.* **199**, 191 (2000).

99. Li, H., Xu, Y., Li, H., and Deng, J.F., *Appl. Catal. A: Gen.* **216**, 51 (2001).

100. Li, H., Xu, Y., and Deng, J.F., *New J. Chem.* **11**, 1059 (1999).

101. Bish, D.L., and Howard, S.A., *J. Appl.Cryst.* **21**, 86 (1988).

102. Coenen, J. W. E., *Appl. Catal.* **75**, 193 (1991).

103. Ruckenstein, E., and Hang Hu, Y. *Appl. Catal. A:Gen.* **183**, 85 (1999).

104. Verhaak, M.J.F.M., Van Dillen, A.J., and Geus, J.W., *J. Catal.* **143**, 187 (1993).

105. Smeds, S., Salmi, T., Lindfors, L.P., and Krause, O., *Appl. Catal. A: Gen.* **144**, 177 (1996).

106. Cesteros, Y., Salagre, P., Medina, F., and Sueiras, J.E., *Appl. Catal. B: Environ.* **25**, 213 (2000).

107. Cesteros, Y., Salagre, P., Medina, F., and Sueiras, J.E., *Appl. Catal. B: Environ.* **22**, 135 (1999).

Marécot, P., Paraiso, E., Dumas, J.M., and Barbier, J., *Appl. Catal.* **74**, 261 (1991).

IV.2.3 Evolución de varios catalizadores de níquel durante la reacción de hidrogenación de 1,6-hexanodinitrilo.

Journal of Catalysis (pendiente de aceptación).

Evolution of several Nickel catalysts during the hydrogenation reaction of 1,6-Hexanedinitrile.

Marc Serra[a], Pilar Salagre[a*], Yolanda Cesteros[a], Francisco Medina[b] and Jesús E. Sueiras[b].

[a] Facultat de Química, Universitat Rovira i Virgili, 1.43005, Tarragona, Spain.
e-mail: salagre@quimica.urv.es
[b] Escola Tècnica Superior d'Enginyeria Química, Universitat Rovira i Virgili,
Av. Països Catalans, 26, 43007, Tarragona, Spain

ABSTRACT

Two bulk nickel catalysts and two Ni-MgO systems were prepared. Were studied their surface modification during the hydrogenation of 1,6-hexanedinitrile in the gas phase at atmospheric pressure in order to correlate it to the activity variation with time. Catalysts before and after the catalytic reaction at different reaction conditions were characterized by different techniques. All catalysts show an evolution of activity until arrive to a constant value of conversion and selectivity. The catalyst obtained after reduction of the catalytic precursor $4C_3B$ (which has solid solution) maintains after 216 h of reaction a conversion of 70% for a selectivity to monoamine of 80%. The metallic area decreases after reaction for all catalysts. However, mainly for catalysts with magnesia, the use of high space velocity facilitates the elimination of reaction products and therefore this gives place to a lower decrease of metallic area and even catalysts almost maintain or increase its BET area values.

Key Words: lifetime studies, nickel catalysts; nickel-magnesia catalysts, adiponitrile; dinitrile; 1,6- hexanedinitrile hydrogenation, 6-aminohexanenitrile.

INTRODUCTION

The hydrogenation of adiponitrile to 1,6-hexanediamine [1-6] is an interesting industrial process in the preparation of Nylon-6,6, and also to obtain 6-aminohexanenitrile [7,8], which is used in the preparation of caprolactam (precursor to Nylon-6) [9-12].

Nitriles hydrogenation products are composed mainly of a mixture of primary, secondary ant tertiary amines [13,14]. Condensation reactions to secondary and tertiary amines can appear when the highly reactive intermediate imine reacts with the primary amine [15,16].

The selectivity of the process can be partially controlled with the catalyst. Thus, mostly primary amines are obtained when Co, Ni and Ru are used [5,6, 17-23]. In the industry, the hydrogenation is performed in liquid phase at high pressure. The Raney Ni is probable the most frequently used catalyst [6,17].

Raney Ni and Raney Co are very active but generally, excess of ammonia is necessary to decrease side reactions leading to secondary and tertiary amines [20-22, 24].

The condensation compounds can remain on the metallic surface and block catalytically active sites [16]. Additionally, Verhaak et al. [25], propose that the deactivation of nickel catalysts in the hydrogenation of acetonitrile is due to the formation of surface nickel carbides and other partial dehydrogenated species, which were strongly adsorbed on the nickel surface and block active sites.

A great number of attempts have been made to replace Raney Ni by a more selective catalyst with less contaminate preparation in the adiponitrile hydrogenation [26-32]. However, it is difficult to find a deactivation resistant nickel catalyst for this reaction due to the causes commented above. In recent studies, we found that nickel-magnesia catalysts show lower amount of high-molecular-weight products than a nickel bulk catalyst for the hydrogenation of 1,4-butanedinitrile [33].

When different Ni-MgO catalysts were tested in the hydrogenation of 1,6-hexanedinitrile, these systems showed at 24 h of reaction high conversion and high selectivity to 6-aminohexanenitrile (around 85%) and 1,6-hexanediamine (100%) at different reaction conditions. We also reported that the crystal morphology of these catalysts could induce the selectivity to monoamine and that the presence of basic magnesia decreases the condensation reactions and favors the elimination of amines and therefore could prevent catalyst deactivation. However, there are some modification of surface properties in the catalyst after reaction [34].

The economic importance to produce 1,6-hexanediamine and especially 6-aminohexanenitrile, is reflected in the contents of the articles published in the last years about this subject [26-34] and mainly in the number of patents registered [3-6, 10, 17-20, 35-40]. We think that more information about the activity evolution of the catalysts at different reaction conditions is needed to confirm that Ni-MgO catalysts are suitable for the industrial hydrogenation of 1,6-hexanedinitrile.

In this work, we propose a study about the evolution of the nickel catalysts characteristics during the adiponitrile hydrogenation process and their influence on the catalytic activity. With this goal two bulk nickel catalysts and two Ni-MgO systems are prepared and

studied for the hydrogenation of 1,6-hexanedinitrile in the gas phase at atmospheric pressure for several days. Catalysts before and after the catalytic reaction at different reaction conditions are characterized by different techniques, in order to explain the differences of activity observed for each catalyst in function of the time and correlate their performances with the structural properties after reaction.

EXPERIMENTAL

Catalysts preparation

The NiO precursor was prepared by means of controlled thermolysis of $Ni(NO_3)_2 \cdot 6H_2O$ at 373 K for 14 days to obtain $Ni_3(NO_3)_2(OH)_4$, which was subsequent calcined at 573 K under an argon atmosphere flow, (referred to as NiOB).

The Raney-nickel catalyst used was a commercial nickel sponge suspension in water (Fluka 99%) and was dried under pure H_2 flow at 453 K for 1h, (referred to as Raney-Ni).

Two NiO/MgO samples were prepared according to the method previously described for $4C_3B$ catalyst precursor [33,41] and for $4C_3C$ catalyst precursor [34] in order to obtain systems with and without solid solution and therefore with different interaction levels between NiO and MgO phases.

The nickel catalysts were obtained by reduction of the precursors above mentioned. The NiOB sample was reduced under pure H_2 at 573 K for 4h (named as NiB) and $4C_3B$ and $4C_3C$ precursors were reduced under pure H_2 at 673 K for 6h (referred to as $R4C_3B$ and $R4C_3C$, respectively).

Characterization methods

BET surface areas were calculated from the nitrogen adsorption isotherms at 77 K using a Micromeritics ASAP 2000 surface analyser and a value of 0.164 nm^2 for the cross-section of the nitrogen molecule.

Powder X-ray diffraction patterns of the samples were obtained with a Siemens D5000 diffractometer using nickel-filtered Cu Kα radiation. This technique was also used to determine the reduction degree (α) of the catalysts by means of the Rietveld method [42].

Temperature-programmed reduction studies (TPR) were carried out in a Labsys/Setaram TG DTA/DSC, equipped with a 273-1273 K programmable temperature furnace. Each sample was first heated at 423 K in an Ar flow until no change of weight was detected. Then, the sample was heated in a 5vol% H_2/Ar flow from 423 K to 1173 K at a rate of 5 K min^{-1}.

Hydrogen chemisorption was measured with a Micromeritics ASAP 2010C equipped with a turbomolecular pump. Samples had been previously reduced under the same conditions as for preparing the catalysts and the hydrogen was analysed at 303 K. The nickel surface area was calculated assuming a stoichiometry of one hydrogen molecule per two surface nickel atoms and an atomic cross-sectional area of 6.49×10^{-20} m^2/Ni atom.

Scanning electron micrographs (SEM), were obtained with a JEOL JSM6400 scanning microscope operating at an accelerating voltage in the range 30-35 kV.

Determination of the catalytic activity

The gas phase hydrogenation of 1,6-hexanedinitrile at atmospheric pressure (1 Torr) was studied in a tubular fixed-bed flow reactor heated by an oven equipped with a temperature control system. The reactor was filled with catalyst (314 mg of Raney-Ni, 400 mg of NiOB, 500 mg of $4C_3B$ and $4C_3C$ samples). These amounts of each one allow to obtain after reduction, the same theoretical amount of Ni.

Reaction products were analysed by an on-line gas-chromatograph HP 5890 equipped with a 30 m "commercial Rtx-5 amine" cappillary column and a flame ionization detector.

Conversion and selectivity were defined by the following equations: conversion (%)= [moles of 1,6-hexanedinitrile consumed] x 100 / [moles of 1,6-hexanedinitrile charged]; selectivity (%) = [moles of one product of reaction] x 100 / [moles of 1,6-hexanedinitrile consumed].

The TOF values for the catalysts were calculated from H_2 chemisorption data as the number of converted molecules of adiponitrile s^{-1} divided by the total number of surface nickel atoms obtained after reaction.

RESULTS AND DISCUSSION

Characterization of catalyst precursors and catalysts before reaction

Table 1 shows some characterization results of the catalytic precursors. More information about the characteristics of $4C_3B$ and $4C_3C$ samples and their corresponding catalysts have been described in recent studies, for $4C_3B$ [33,41], and for $4C_3C$ [34].

TABLE 1

Characterization of the catalytic precursors

	NiOB	$4C_3B$	$4C_3C$
Crystalline phases (XRD)	NiO	NiO-MgO solid solution	NiO
Crystallite sizes (nm)[a]	27.1	35.2	19.7
Surface area (m^2g^{-1})[b]	84.9	36.4	85.3
T_R (K) (TPR) [b]	523	604	523

[a] Using Scherrer equation.

[b] Using BET area method.

[c] T_R = initial reduction temperature, obtained by TPR experiments.

The preparation procedure used to obtain the NiOB sample allowed to obtain a solid with very homogeneous octahedral morphology. This result is in agreement with that obtained for other NiO preparations from the same $Ni_3(NO_3)_2(OH)_4$ precursor [33]. However in this new procedure a higher surface area has been obtained (84.9 $m^2 g^{-1}$), probably due to the use of an argon atmosphere flowing throw the sample during the calcination process. The argon flow favors the efficient elimination of the decomposition products and therefore the

agglomeration is lower. These phenomena should be similar to that observed in the preparation of the $4C_3C$ catalytic precursor [34].

The SEM micrographies confirm that NiOB, $4C_3B$, $4C_3C$ precursors have octahedral morphology. This defined morphology was expected since all samples were prepared through the intermediate specie $Ni_3(NO_3)_2(OH)_4$.

When this phase has been observed as a pure compound in the decomposition of nickel nitrate (alone or in the magnesia presence) homogeneous octahedral NiO particles have been always obtained after calcination [33,34].

TABLE 2

Characterization of the catalysts before and after reaction at different reaction conditions.

Catalysts	Reaction conditions			Crystall Ni sizes (nm)[a]	Metallic area (m^2g^{-1})[b]	Surface area (m^2g^{-1})[c]	Reduction degree α[d]
	H_2/ADN ratio	Space velocity (h^{-1})	Reaction temp. (K)				
Raney-Ni		Fresh		9.2	31.0	72.8	1
1)	178	23873	423	8.8	14.7	26.5	1
2)	163	34139	413	9.5	7.5	24.5	1
NiB		Fresh		206.0	0.31	2.4	1
1)	178	1790	423	190.0	0.07	1.1	1
2)	178	7162	423	186.6	0.14	2.6	1
$R4C_3B$		Fresh		10.1	16.1	44.6	0,65
1)	178	1790	423	13.9	1.3	13.6	0,60
2)	178	7162	423	12.1	8.3	41.8	0,64
$R4C_3C$		Fresh		132.0	1.8	20.5	1
1)	178	1790	423	120.9	0.4	26.5	1
2)	178	7162	423	117.1	1.4	29.4	1

[a] Using Scherrer equation

[b] Using BET area method.

[c] Metal surface area, (m^2g^{-1} catalyst), calculated from chemisorbed H_2.

[d] Reduction degree obtained after reduction and using Rietveld method [42].

Table 2 shows several characterization results for the four catalysts before reaction referred to as fresh catalysts. The Raney-Ni, NiB and $R4C_3C$ catalysts have crystalline nickel as single phase and

A)

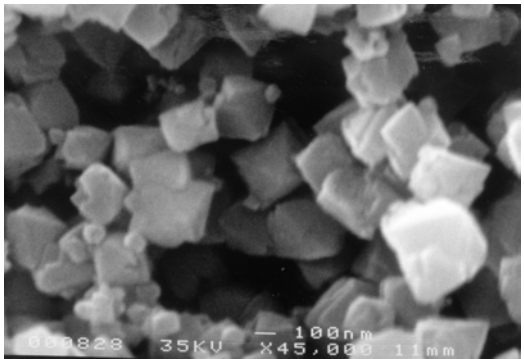

show total reduction. In contrast, catalyst R4C_3B shows a partial reduction (α=0,65) as expected from the lower reducibility of the 4C_3B precursor observed by TPR, which is related with the higher interaction between NiO and MgO phases when form a solid solution [34].

FIG. 1. Scanning electron micrographs of NiOB precursor (a) and its corresponding catalyst NiB (b).

The NiOB precursor has similar initial reduction temperature than 4C_3C (table 1). However, after reduction NiB catalyst shows lower surface area, metallic area, and higher crystallite size than catalyst R4C_3C. This is related to the higher sintering of metallic particles suffered by NiB catalyst, in spite of using a lower reduction

B) 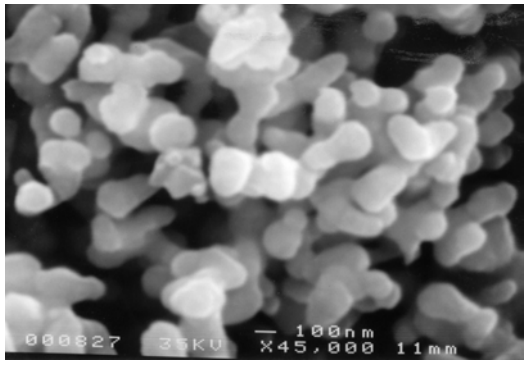

temperature (573 K) in the preparation of this catalyst (Fig. 1).

The main difference in 4C_3C precursor respect to the NiOB precursor is the presence of magnesia, which makes more difficult the agglomeration for catalyst R4C_3C.

Lifetime studies of catalysts

In order to obtain information about the influence of the type of products obtained on the catalyst characteristics and activity for the adiponitrile hydrogenation during the first hours of reaction, we designed two catalytic experiments: one at high conversion and the other at lower conversion. Different activities were obtained modifying reaction temperature, space velocity, and the H_2/Adiponitrile (ADN) ratio.

The products obtained for each conversion depends on the catalyst and too on the reaction conditions [34]. High conversion is favored at high temperature, high H_2/ADN ratio and at low space velocity. In these conditions a catalyst active in the adiponitrile hydrogenation usually leads to the formation of azacycloheptane followed by 1,6-hexanediamine and 6-aminohexanenitrile in this order. Also, some cracking products and sometimes 3,4,5,6-tetrahydro-2H-azepine (THAPN) can be produced. On the other hand, the use of high space velocities and lower H_2/ADN ratio decrease the conversion values but increases the amount of the less hydrogenated specie (6-aminohexanenitrile). The compound THAPN also increases slightly.

After reaction, catalysts were characterized, and the results are shown in table 2. This study will be very interesting to evaluate the industrial use of the recently obtained Ni-MgO catalysts which showed high selectivity to 6-aminohexanenitrile (around 80%) the first 24 hours [34].

In the experiments designed, the space velocity was higher in Raney-Ni experiments to maintain the same amount of active phase for all catalysts.

1) High conversion: Reaction temperature (423 K), ADN vapor pressure (4,28 torr), H_2/ADN ratio (178) and space velocity (23873 or 1790h^{-1} for Raney-Ni and the others catalysts respectively).

2) Lower conversion: Reaction temperature (413 K), ADN vapor pressure (2,34 torr), H_2/ADN ratio (163), and space velocity (34139 h^{-1}) for Raney-Ni. Reaction temperature (423 K), ADN vapor pressure (4,28 torr), H_2/ADN ratio (178) and space velocity (7162 h^{-1}) for the others catalysts.

The different reaction conditions in experiment 2 for Raney-Ni respect to the other catalysts, was made in order to increase the 6-aminonitrile selectivity. This is possible at lower conversion, and therefore it was necessary to decrease the reaction temperature and H_2/ADN ratio, maintaining a higher space velocity. These reaction conditions have been obtained using hydrogen diluted with argon. Therefore, there is a decrease in the hydrogen amount of the total flow (10% H_2, 90% Ar). Besides a decrease of adiponitrile vapor pressure has been also necessary to control the conversion descent.

A) Raney-Ni catalyst

Figure 2 shows the lifetime studies obtained for Raney-Ni catalyst at the two different activity conditions:

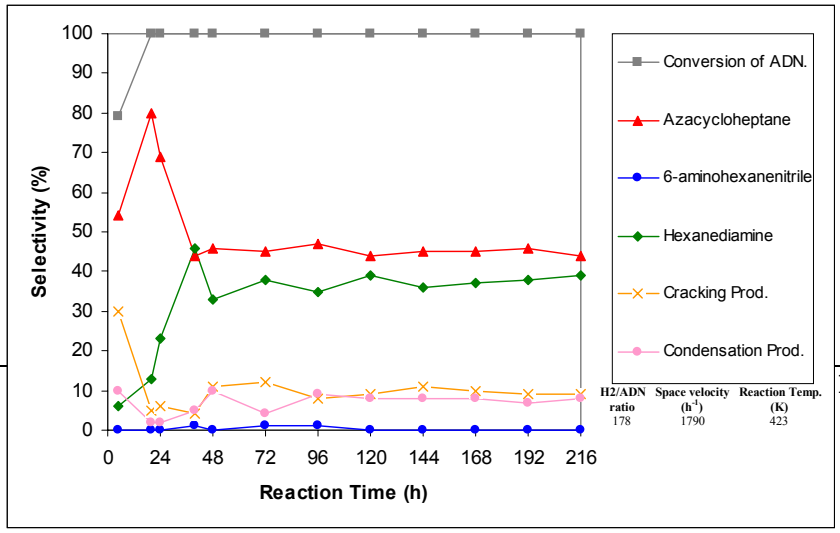

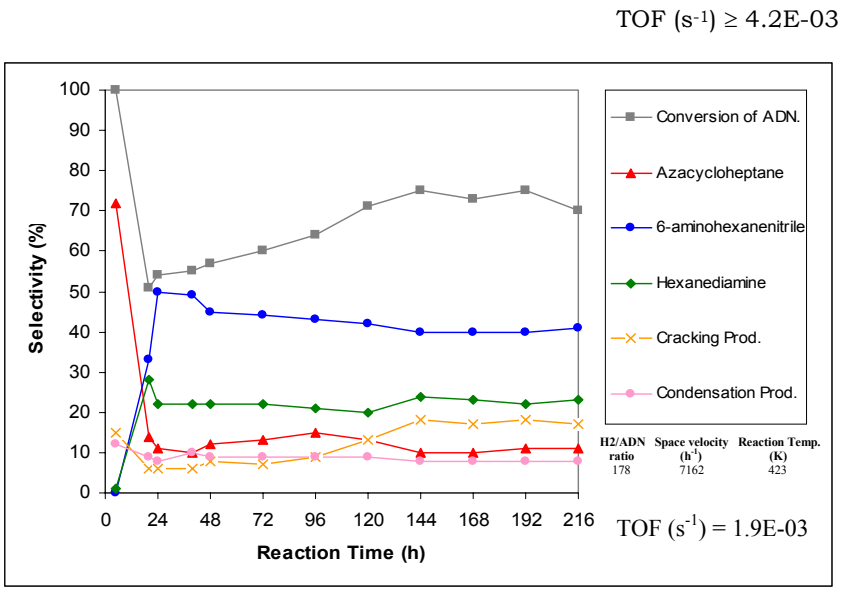

Fig. 2. Lifetime studies for Raney-Ni catalyst at two different reaction conditions.

1) Conditions of higher conversion.

The total conversion only was obtained after 24 hours of reaction. After this time, conversion and selectivity were constant. At 5 h, there is a partial conversion of adiponitrile (80%) and selectivity to azacycloheptane of 53%, however there is a high amount of cracking products (30%). This partial conversion together to the cracking compounds obtained in the first hours, can be explained by a strong interaction of the reaction products with some active sites. This fact probably produces a partial blockade in the catalyst and favors the cracking and the intermolecular amine-imine condensation reactions.

The effect of this initial blockade on the catalyst surface probably is the partial decoration of Ni particles. This is in agreement with the decrease of surface and metallic area observed for this catalyst

after reaction (Table 2). The consequence is a certain loss of activity for the more active centers, which still have high capacity of conversion but the interaction reactive-active site is lower. This is in agreement with the activity results after 24 hours, total conversion, decrease of cracking and condensation products and high selectivity to azacycloheptane and hexanediamine.

2) Conditions of lower conversion.

During the first 22 hours there is a high decrease in the conversion value (from total conversion to 50%). However, after 24 h, there is an increase of the conversion value, which is stabilized at 120 h at around 70 %. The selectivity to the main products is: 40% of 6-aminohexanenitrile and 22% of hexanediamine. Also there is an important amount of cracking products (17%).

At the conditions of partial conversion, the results obtained from the characterization of the catalyst after reaction show a higher decrease of surface and metallic area than in the more active conditions, which confirms a more important decoration of the small Ni particles (Table 2). In this system, the use of a higher space velocity does not seem to favor the elimination of condensation products in the first 22 h. This could be probably related to a more important influence of a diluted flow on the activity (10% of H_2 in total gas). The use of argon decreases the hydrogenating ability of system [33], and this could favor the condensation reactions, because hydrogenation and condensation reactions are competing. However, independently of the gas used, a higher space velocity can favor the elimination of the more volatile condensation products and, then, the conversion increases slightly with time. This explains the slight conversion increase detected after 24 h of reaction.

In both experiments, when a stable value of conversion is obtained, the selectivity is also constant. The TOF values (given in Fig. 2) confirm that the catalyst is more active at reaction conditions 1 than reaction conditions 2. Both results corroborate the difficulties to obtain high selectivity to monoamine for this catalyst [34].

B) NiB catalyst

Figure 3 shows lifetime studies obtained for NiB catalyst at the two different reaction conditions.

1) Conditions of higher conversion.

There is an important decrease of the conversion in three steps. For each step, conversions values of 90, 60 and 15% seem to be stable for intervals of time between 0-48, 72-144 and 168-216 hours, respectively.

The selectivity also changes with the time and the selectivity to 6-aminohexanenitrile increases progressively for each step. From 72 h, high amounts of 6-aminohexanenitrile (70%) are obtained. This value increases until 85% between 168-216 h. The highest selectivity is obtained at a conversion of 15%.

The great loss of activity is probably related to the higher difficulty to remove the basic reaction products in a catalyst with lower hydrogenation activity due to its high Ni particle size (206 nm). The reaction products can be more easily eliminated using Ni/MgO systems due to presence of the basic sites, or in Raney-Ni catalyst, which has very small nickel particles.

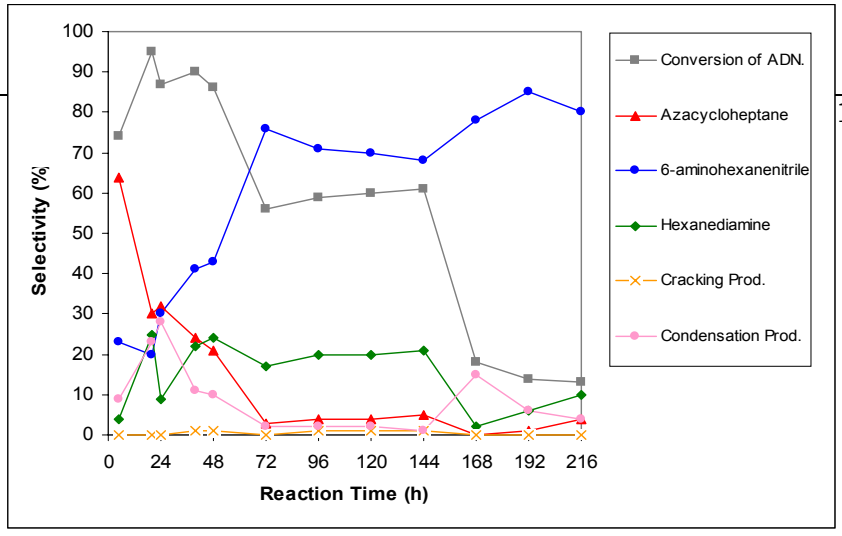

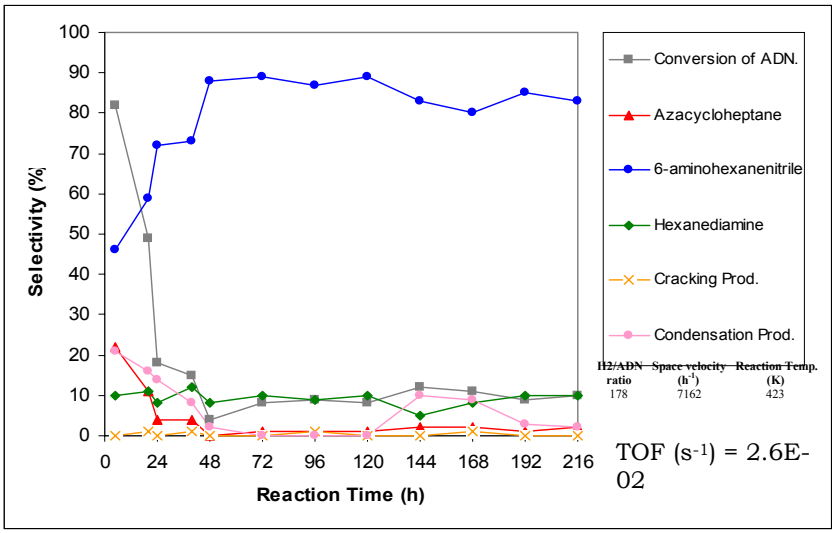

Fig. 3. Lifetime studies for NiB catalyst at two different reaction conditions.

At these conditions tested, the formation of condensation product is favored and a progressive decoration of the nickel particles is obtained. The decrease of surface and metallic area after reaction (Table 2) corroborate this loss of activity.

2) Conditions of lower conversion.

Under these reaction conditions with lower hydrogenation ability, conversion decreases drastically in the first 24 hours, but

between 48-72 hours is stabilized (around 10%). At this time, the selectivity to 6-aminohexanenitrile becomes almost constant (80-90%). After reaction, there is also a decrease of metallic area (Table 2). However, the decrease is lower than at the previous reaction conditions.

The higher space velocity used at conditions 2 (7162 h^{-1}) than 1 (1790 h^{-1}) probably hinders the hydrogenation reaction but the elimination of products is easier. A slight increase of BET area value, and a decrease of nickel particle size have been also observed for the used catalyst. Therefore, the use of higher hydrogen flow (higher space velocity) probably produces a disagglomeration of nickel particles during reaction.

The SEM micrograph of the NiB catalyst used in the first conditions shows a similar sintering of nickel particles than for fresh catalysts, but for NiB catalyst after reaction conditions 2 there is a lower agglomeration than before reaction. This observation explains the BET surface results.

This catalyst shows similar TOF values (magnitude order of 1E-03) for all reaction conditions, but higher TOF than the other catalysts. This indicates that the accessible metallic centers are very active.

In order to increase the activity, other reaction conditions have been used. For example, increasing the reaction temperature to 473K and the H_2/ADN ratio to 596, decreasing the ADN vapor pressure at 0.4 torr and maintaining the space velocity at 7162 h^{-1}. At the first 5 h this catalyst shows a conversion around 100%. However, after 24 h the conversion values oscillate around 10%. The selectivity evolves until obtain a 70% of 6-aminohexanenitrile. In general, independently of the

reaction conditions tested, this catalyst has not achieved high conversions. This fact could be related due to their low metallic area.

C) R4C$_3$B catalyst

Figure 4 shows the lifetime studies obtained for catalyst R4C$_3$B at different activity conditions.

1) Conditions of higher conversion.

The performance of this catalyst is very similar to Raney-Ni and a partial conversion (75%) was obtained in the first hours (22 h). This fact can be explained by a strong interaction of the reaction products with some active sites. Therefore, the use of a low total flow for catalyst R4C$_3$B can favor an important initial deactivation. The nickel decoration originated in the initial time probably hinders the access to the active sites, but with the space velocity used, the reaction is possible and a total conversion can be obtained from 22 h.

The results of surface characterization (Table 2) show a decrease of surface and metallic area (13.6 and 1.3 m^2g^{-1}) respect to the fresh catalyst (44.6, 16.1 m^2g^{-1} for BET and metallic area), while the nickel crystallite size increases after reaction, from 10.1 to 13.9 nm. The decoration of nickel particles and its agglomeration can explain these results.

When the 100% of conversion is achieved, the high selectivity to azacycloheptane (around 60%) and the small amounts of cracking products obtained are related with the low space velocity and the moderate reaction temperature used [34].

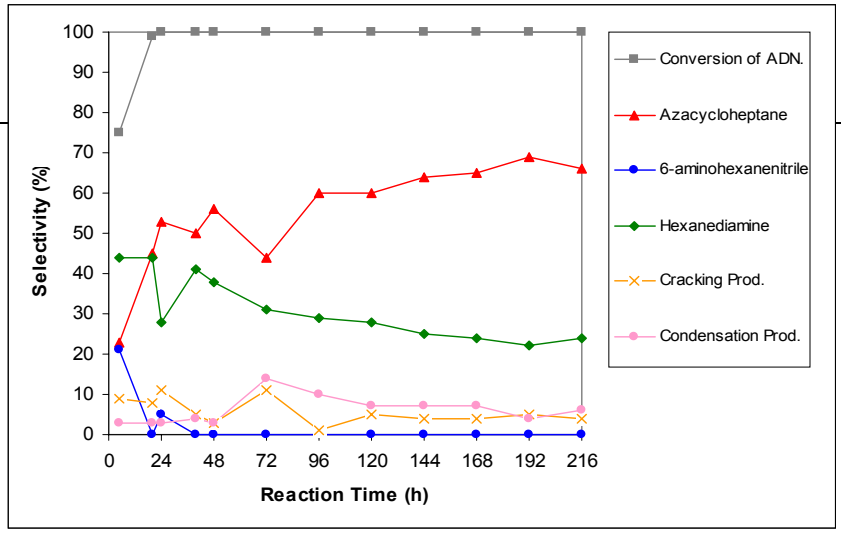

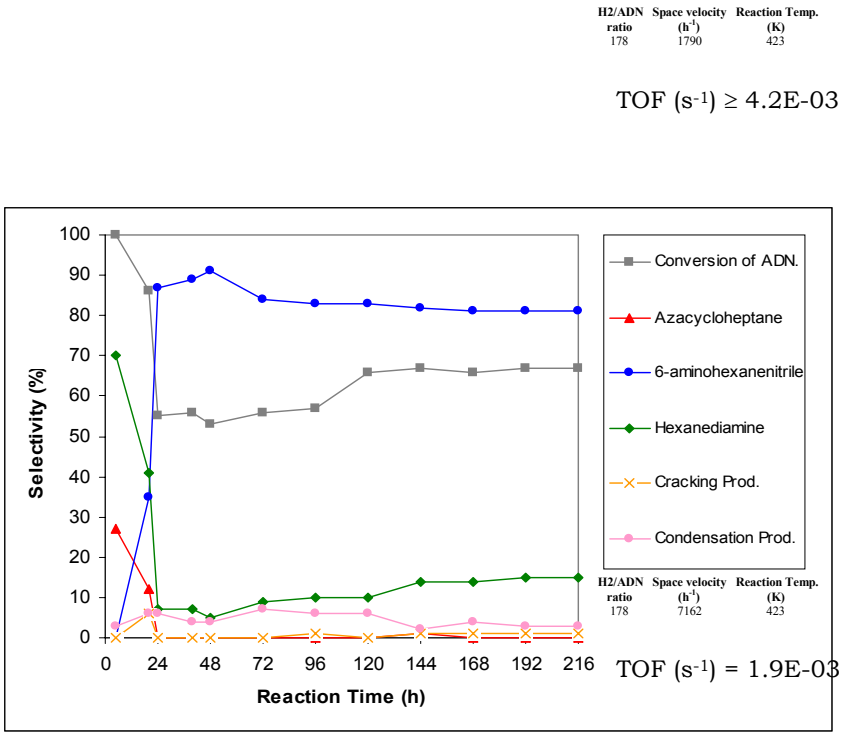

Fig. 4. Lifetime studies for R4C$_3$B catalyst at two different reaction conditions.

2) Conditions of lower conversion.

In the first 24 hours there is an important decrease of the conversion value from 100% down to 55%, followed by a slight increase until stabilization to near 70% at 96 hours. On the other hand, the expected high selectivity to monoamine does not almost vary from 24 hours, arriving above 80%. This selectivity behavior was correlated with the presence of certain octahedral morphology, which seems to induce a higher selectivity to monoamine [34].

For this catalyst, the high space velocity used at these conditions prevents the reactive access to nickel centers after these have been decorated in the initial time and allows to explain its lower activity when compared with fresh catalyst. However, the use of higher space velocity favors the elimination of the lower-weight molecular condensation products, and therefore this catalyst shows similar surface area (41.8 m^2g^1), lower decrease of metallic area (8.3 m^2g^{-1}) but lower conversion than at the reaction conditions 1.

The most significant information from micrographs of catalyst $R4C_3B$ after the 1 and 2 reaction conditions is the better resolution of octahedral morphology observed after reaction conditions 2, similar than previously observed after short reaction time [34].

D) R4C$_3$C catalyst

Figure 5 shows the lifetime studies obtained for catalyst $R4C_3C$ at different activity conditions.

1) Conditions of higher conversion.

As in previous catalysts tested, initially, there is a lower conversion (around 30%), but at 72 h the conversion is 90% and finally arrive to 100% after 120 hours. The partial active center blockade is also corroborated with the characterization results (Table 2) for this catalyst. However, the low hydrogen flow used is probably sufficient and allows to remove some light condensation products, together to the with higher residence time, which allows the reagent to arrive until the partially blocked active centers and therefore the conversion with the time arrives to 100%.

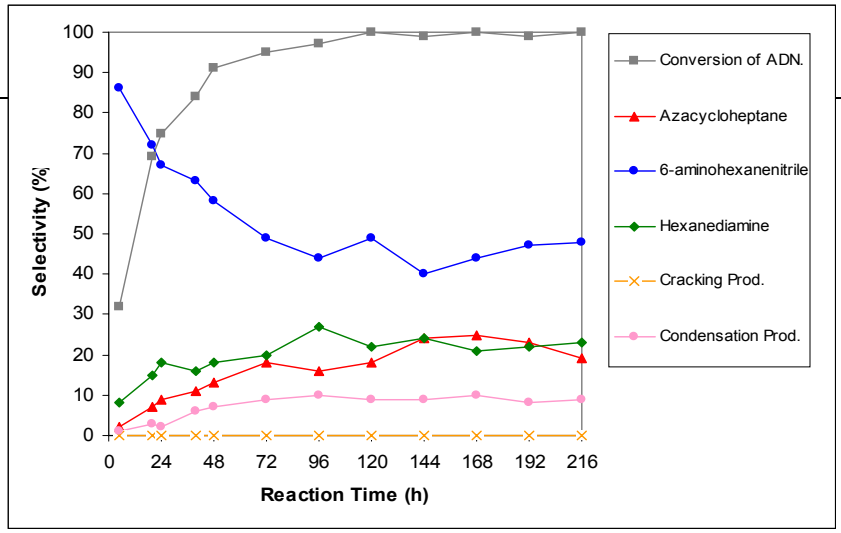

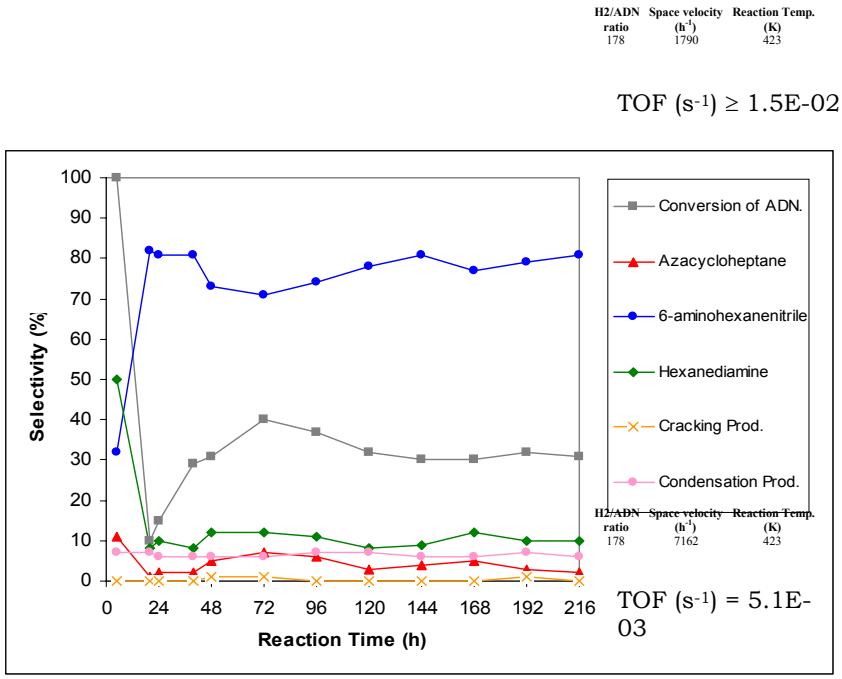

Fig. 5. Lifetime studies for R4C$_3$C catalyst at two different reaction conditions.

The selectivity values are stable enough from 72-96 hours showing a value around 45% to 6-aminohexanenitrile, similar amount to hexanediamine and azacycloheptane (20% respectively) and a 10% of condensation products.

The higher selectivity to 6-aminohexanenitrile observed (a less hydrogenated product) for catalyst R4C$_3$C than for catalyst R4C$_3$B, at reaction conditions 1, indicates a lower activity for catalyst R4C$_3$C than R4C$_3$B. This can be related to their lower metallic area.

2) Conditions of lower conversion.

In the first 24 h there is an important decrease of the conversion value from 100% to 10%, followed by a slight increase until a certain stabilization near 30% at 48 h. The selectivity to monoamine is high (around 80%) and constant during all experiment.

The higher conversion lost for this catalyst at the conditions tested could be related with its small initial metallic area (1.8 m^2g^{-1}) and high Ni particle sizes (132 nm). The selectivity to 6-aminohexanenitrile is similar than obtained for catalyst A under the same conditions.

The results of surface characterization for $R4C_3C$ catalyst after reaction conditions (1 and 2), show for both experiments an increase of the BET area values (26.5 and 29.4 m^2g^{-1} respectively), whereas the metallic area decrease (0.4 and 1.4 m^2g^{-1}) respect to the BET and metallic values obtained before reaction (20.5 and 1.8 m^2g^{-1} respectively).

This fact was also observed for NiB catalyst and could be explained as a result of the a disagglomeration of Ni and MgO particles during reaction and some decoration on nickel particles. The lower decrease of metallic area observed when reaction conditions 2 has been used is related with the higher space velocity, which disagglomerate particles and minimize the retention of reaction products and therefore the decoration is lower.

The SEM micrographs for this catalyst after reaction conditions show the presence of more disagglomerate particles than before reaction especially when the reaction conditions 2 has been used.

CONCLUSIONS

Bulk nickel and nickel-magnesia catalysts tested in the adiponitrile hydrogenation during 216 hours, showed modifications in its activity with time. This evolution has been related with its surface properties after reaction for each catalyst.

All catalysts show a decrease of metallic area after reaction. This fact is explained by a partial decoration of the nickel particles, mainly in the first hours of reaction due to different reasons depending on the catalyst. For the Raney-Ni catalyst it is due to the strong interaction of reactive and products on the small nickel particles and in the other catalysts for a higher competition between condensation and hydrogenation reactions. However, the use of high space velocity using allows better eliminate the most volatile condensation products, and this explains the lower decrease of metallic area for NiB, $R4C_3B$ and $R4C_3C$ catalysts.

On the other hand, the higher decoration of Raney-Ni particles at the conditions of partial activity is due to the use of less hydrogenating conditions.
Catalyst NiB and $R4C_3C$ suffer a high sintering effect during the reduction, but the use of high space velocity during reaction allows to disagglomerate some nickel particles and therefore to increase the BET value and decrease its nickel crystal size.

The TOF values obtained for $R4C_3B$, $R4C_3C$ and NiB catalysts are higher than for Raney-Ni catalyst and, so the few active centers and specially for Ni catalyst, are very active. However, the lower metallic area leads to lowest conversions for NiB catalyst.

Finally, these lifetime studies show that $R4C_3B$ and $R4C_3C$ catalysts are usable for the catalytic industrial manufacture of 6-aminohexanenitrile. However, a key point will be to choose the

optimum reaction conditions in order to obtain the desired products, maintaining the maximum surface and metallic area values.

REFERENCES

108. Weissermel, K., and Arpe, H.J. *"Industrial Organic Chemistry"*, Verlag Chemie, Berlin, 1978.

109. Volf, J., and Pasek, J., *"Catalytic Hydrogenation, Studies in Surface Science and Catalysis"* (L.Cervený Ed.), Vol. 27. Elsevier, Amsterdam, 1986.

110. Vandenbooren, F., Bosman, H., and Van der Spoel, J., WIPO Patent WO9426699A1, 1994 (DSM N.V.).

111. Cordier, G., Fouilloux, P., Laurain, N., and Spindler, J.F., WIPO Patent WO9518090A1, 1995 (Rhone Poulenc Chimie).

112. Schnurr, W., Voit, G., Flick, K., Melder, J. P., Fischer, R., and Harder, W., WIPO Patent WO9737964A1 1997 (BASF AKTIENGESELLSCHAFT).

113. Koch, T. A., Krause, K. R., and Sengupta, S. K., WIPO Patent WO9843940A1, 1998 (E.I. DuPont de Nemours and Company).

114. Diamond, S.E., Mares F., and Szalkiewicz, A., EPO Patent EP077911A1, 1983 (Allied Corporation).

115. Sanchez, K. M., EPO Patent EP642493B1, 1996 (E. I. DuPont de Nemours and Company).

116. Harrison., C.R., *"Catalysis and Chemical Processes"* (R.Pearce and W.R. Patterson, Eds), Chapter 7, 1981.

117. Brunelle, J. P., Seigneurin, A., and Sever, L., WIPO Patent WO005203A1, 2000 (Rhodia Fiber and Resin Intermediates).

118. Sheldon, R., *Green Chem.* **2**(1), G1 (2000).

119. Clark, J., *Green Chem.* **1**(1), 1 (2000).

120. Mares, F., Galle, J.E., Diamond, S.E., and Regina, F. J., *J. Catal.* **112**, 1 (1988).

121. Huang, Y., and Sachtler, W. M. H., *Appl. Catal A: Gen.* **182**, 365 (1999).

122. Augustine, R.L., *Catal. Rev.* **13**, 285 (1976).

123. Prins, R., *Catal. Today* **37**, 103 (1997).

124. Boschat, V., and Brunelle, J. P., WIPO Patent WO027806A1, 2000 (Rhodia Fiber and Resin Intermediates).

125. Harper, M. J., WIPO Patent WO027526A1, 2000 (E.I. DuPont de Nemours and Company).

126. Diamond, S.E., Mares F., and Szalkiewicz, A., EPO Patent EP077911A1, 1983 (Allied Corporation).

127. Frank, G., and Neubauer, G., Germany Patent DE3402734A1, 1984 (BASF AKTIENGESELLSCHAFT).

128. Greenfield, H., *Ind. Eng. Chem. Prod. Res. Develop.* **6**, 142 (1967).

129. Pasek, J., Kostova, N., and Dvorak, B., *Collect. Czech. Chem. Comunn.* **46**, 1011 (1981).

130. Huang, Y., and Sachtler, W.M.H., *J. Catal.* **184**, 247 (1999).

131. Schowoegler, E. J., and Adkins, H., *J. Am. Chem. Soc.* **61**, 3449 (1939).

132. Verhaak, M. J. F. M., Van Dillen, A. J., and Geus, J. W., *J. Catal.* **143**, 187 (1993).

133. Medina, F., Salagre, P., Sueiras, J.E., and Fierro, *J.L.G., J. Catal.* **142**, 392, (1993).

134. Medina, F., Salagre, P., Sueiras, J.E., and Fierro, J.L.G., *J. Mol. Catal.* **81**, 363, (1993).

135. Medina, F., Salagre, P., Sueiras, J.E., and Fierro, J.L.G., *J. Chem. Soc. Faraday Trans.* **89**(18), 3507 (1993).

136. Medina, F., Salagre, P., Sueiras, J.E., and Fierro, J.L.G., *J. Chem. Soc. Faraday Trans.* **89** (21), 3981 (1994).

137. Yu, X., Li, H., and Deng, J.F., *Appl. Catal. A: Gen.* **199**, 191 (2000).

138. Li, H., Xu, Y., Li, H., and Deng, J.F., *Appl. Catal. A: Gen.* **216**, 51 (2001).

139. Li, H., Xu, Y., and Deng, J.F., *New J. Chem.* **11**, 1059 (1999).

140. Serra, M., Salagre, P., Cesteros, Y., Medina, F., and Sueiras, J.E., *J. Catal.* **197**, 210 (2001).

141. Serra, M., Salagre, P., Cesteros, Y., Medina, F., and Sueiras, J.E., *J. Catal.* **209** (2002). In press

142. Leconte P., WIPO Patent WO9959962A1, 1998 (Rhodia Fiber and Resin Intermediates).

143. Boschat, V., Leconte, P., Rochette, D., and Sever, L., WIPO Patent WO9926917A1, 1999 (Rhodia Fiber and Resin Intermediates).

144. Luyken, H., Ohbach, F., Ansmann, A., Bassler, P., Fischer, R., Melder, J. P., Merger, M., Rehfinger, A., Voit, G., and Achhammer, G., WIPO Patent WO005191A1, 2000 (BASF AKTIENGESELLSCHAFT).

145. Luyken, H., Ohbach, F., Ansmann, A., Bassler, P., Fischer, R., Melder, J. P., Merger, M., Rehfinger, A., Voit, G., and Achhammer, G., WIPO Patent WO012459A1, 2000 (BASF AKTIENGESELLSCHAFT).

146. Fischer, R., Bassler, P., Luyken, H., Ohbach, F., Melder, J. P., Merger, M., Ansmann, A., Rehfinger, A., and Voit, G., WIPO Patent WO012460A1, 2000 (BASF AKTIENGESELLSCHAFT).

147. Ionkin, A. S., Ziemecki, S. B., Koch, T. A., and Bryndza, H. E., WIPO Patent WO064862A3, 2000.

148. Serra, M., Salagre, P., Cesteros, Y., Medina, F., and Sueiras, J.E., *Solid State Ionics* **134**, 229 (2000).

149. Bish, D. L., and Howard, S. A., *J. Appl. Cryst.* **21**, 86 (1988).

150.